

THESIS

A STUDY OF FUMED SILICA PARTICLE DEAGGLOMERATION ASSOCIATED WITH  
INSTRUMENT SAMPLING TECHNIQUES

AND

A COMPARISON OF NIOSH 7402 AND THE TSAI DIFFUSION SAMPLER FOR  
COLLECTING AND ANALYZING CARBON NANOTUBES

Submitted by

Jared Khattak

Department of Environmental and Radiological Health Sciences

In partial fulfillment of the requirements

For the Degree of Master of Science

Colorado State University

Fort Collins, Colorado

Summer 2018

Master's Committee:

Advisor: Candace Su-Jung Tsai

Stephen Reynolds  
Shantanu Jathar

Copyright by Jared Khattak 2018

All Rights Reserved

## ABSTRACT

### A STUDY OF FUMED SILICA PARTICLE DEAGGLOMERATION ASSOCIATED WITH INSTRUMENT SAMPLING TECHNIQUES

AND

### A COMPARISON OF NIOSH 7402 AND THE TSAI DIFFUSION SAMPLER FOR COLLECTING AND ANALYZING CARBON NANOTUBES

Accurate characterization of contaminant exposures is critical in ensuring worker safety. Worker exposures are commonly characterized by area monitoring and personal samples. This research includes two parts, which study real time instrument measurements and personal sampling methods for exposure assessment.

Real time instruments (RTIs) are used to assess concentrations of airborne particles in manufacturing facilities. These instruments often contain a cyclone, and previous studies have shown that the cyclone may cause measurement variations by dispersing agglomerated particles. This mechanism is thought to increase particle concentrations and decrease particle size. To determine the cyclone effect in this study, three RTIs were evaluated; the scanning mobility particle sizer (SMPS), fast mobility particle sizer (FMPS), and the optical particle sizer (OPS). The SMPS and FMPS contain a cyclone, the OPS does not. Nanoparticles were generated and sampled through pouring and automatic stirring inside a glovebox enclosure. After particles were generated, the glovebox was thoroughly cleaned and measurements were taken in the glovebox. For both generation methods, the SMPS and FMPS recorded an average concentration of  $1.2 \times 10^3$  particles/cm<sup>3</sup> and  $1.7 \times 10^4$  particles/cm<sup>3</sup> more after runs where the cyclone was used than when

the cyclone was not used. The OPS, which does not contain a cyclone, recorded minimal differences during the measurement period after the glovebox was cleaned when the cyclone was used and not used on the other instruments. This result indicated that the measured nanoparticle concentrations increased with cyclone use. The results of this study indicate that the cyclone does influence the concentrations recorded by RTIs, and should be cleaned to ensure accurate measurements.

The personal sampling methods evaluated were the NIOSH 7402 method for collecting and analyzing Carbon Nanotubes (CNTs) and the Tsai Diffusion Sampler (TDS) method for sampling CNTs. To evaluate each sampling method, CNTs were generated in a small enclosure inside of a glovebox; CNTs were generated by manual stirring. RTIs also sampled during each experiment to provide an estimate of airborne CNT concentrations. Airborne concentrations were estimated using the particle counts from TEM grid samples prepared using both methods. The majority of CNT structures collected by the TDS were individual fibers and clusters smaller than one micron in diameter. The NIOSH 7402 sampler primarily collected larger agglomerates, with the majority of collected particles being larger than two microns in diameter. The average estimated airborne concentrations calculated from the TDS and 7402 method particle counting were 5,200 fibers/cm<sup>3</sup> and 59 fibers/cm<sup>3</sup> respectively. During the experiments the SMPS recorded an airborne concentration of 1,100 particles/cm<sup>3</sup> and the OPS measured an airborne concentration of 33 particles/cm<sup>3</sup>. Because the concentrations measured by the RTIs significantly exceeded the estimated concentrations derived from the NIOSH 7402 method, it is recommended that the TDS sampler be used as the concentrations derived from this sampler would warrant a more conservative approach to worker safety.

## ACKNOWLEDGEMENTS

I would like to thank my advisor Dr. Candace Tsai for mentoring me throughout this process, and allowing me to grow both personally and academically. I would like to thank my committee members, Dr. Stephen Reynolds and Dr. Shantanu Jathar, for assisting me in writing and revising my thesis. I would also like to thank Daniel Theisen and Nara Shin for assisting me with experiments. Lastly, I would like to thank the Mountain and Plains Education and Research Center for funding my education and research (Grant # - T420H009229)

## TABLE OF CONTENTS

ABSTRACT .....	ii
ACKNOWLEDGEMENTS.....	iv
LIST OF TABLES.....	vi
LIST OF FIGURES.....	vii
<b>PART ONE: A STUDY OF FUMED SILICA PARTICLE DEAGGLOMERATION ASSOCIATED WITH INSTRUMENT SAMPLING TECHNIQUES.....</b>	<b>1</b>
CHAPTER 1: INTRODUCTION.....	2
CHAPTER 2: METHODOLOGY.....	5
2.1 Process.....	5
2.2 Evaluation of Real Time Instrument Measurements.....	7
2.3 Evaluation of Particle Images taken by Electron Microscopy.....	8
2.4 Statistical Analysis.....	8
2.5 Materials and Instrumentation.....	9
CHAPTER 3: RESULTS AND DISCUSSION.....	11
3.1 Cyclone Effect during Experimental Process.....	11
3.2 Effect of Particle Generation Method.....	12
3.3 Post-cleaning Concentration and Distribution Results.....	12
3.4 Comparison of Pre-Experiment and Post-Cleaning Concentrations.....	18
3.5 TEM and SEM Size Distribution Analysis.....	19
CHAPTER 4: CONCLUSION.....	22
REFERENCES.....	23
APPENDIX A.....	24
APPENDIX B.....	28
LIST OF ACRONYMS.....	29
<b>PART TWO: A COMPARISON OF NIOSH 7402 AND THE TSAI DIFFUSION SAMPLER FOR COLLECTING AND ANALYZING CARBON NANOTUBES.....</b>	<b>30</b>
CHAPTER 1: INTRODUCTION.....	31
CHAPTER 2: METHODOLOGY.....	33
2.1 Process.....	33
2.2 Evaluation of Carbon Nanotube Collection.....	34
2.3 Estimation of Airborne Fiber Concentration.....	35
CHAPTER 3: RESULTS AND DISCUSSION.....	36
3.1 Particle Counting and Concentration Extrapolation.....	36
3.2 Qualitative Filter Analysis by SEM.....	39
3.3 Real-Time Instrument Measurements.....	41
CHAPTER 4: CONCLUSION.....	43
REFERENCES.....	45
LIST OF ACRONYMS.....	46

LIST OF TABLES

Table 1-1- Average Total Particle Number Concentration for All Runs.....15  
Table 1-2- Paired t-test results between runs with and without cyclone after glovebox  
cleaning.....16  
Table 2-1- Number of particles collected by each sampler in each size category .....39

LIST OF FIGURES

Figure 1-1 – Experimental designs for both particle generation methods.....6  
Figure 1-2 – Experimental process diagram.....7  
Figure 1-3 – Average particle count measured by the RTIs during all stirring process runs.....17  
Figure 1-4 – Average particle count measured by the RTIs during all pouring process runs.....18  
Figure 1-5 – Electron microscopy images.....21  
Figure 1-S1 – Average particle cumulative percentage measured by the SMPS for all experimental runs.....24  
Figure 1-S2 – Average particle cumulative percentage measured by the FMPS for all experimental runs.....25  
Figure 1-S3 – Average particle cumulative percentage measured by the SMPS after the glovebox was cleaned for all runs.....26  
Figure 1-S4 – Average particle cumulative percentage measured by the FMPS after the Glovebox was cleaned for all runs.....27  
Figure 1-S5 – Average Concentration over Time for all experiments.....28  
Figure 2-1 – Experimental setup for CNT generation .....33  
Figure 2-2 – Equation used for airborne concentration estimation .....35  
Figure 2-3 – TEM images of sample grids .....38  
Figure 2-4 – Histogram of percentage of fiber structures from TEM images collected by each sampler at each size category .....39  
Figure 2-5 – Examples of filter samples taken by SEM .....41  
Figure 2-6 – Particle concentration over time measured by the real-time instruments .....42

PART ONE:

A STUDY OF FUMED SILICA PARTICLE DEAGGLOMERATION ASSOCIATED WITH  
INSTRUMENT SAMPLING TECHNIQUES

## CHAPTER 1: INTRODUCTION

Materials manufactured as a powder often exist in two forms; as a primary particle and as an agglomerate or aggregate of many particles. Primary particles are singular particles that are often less than one micron in diameter, while agglomerate or aggregate particles are a group of primary particles attached to each other (Hartley et al. 1985; Corn 1961). These agglomerates are held together with weak intermolecular forces such as Van der Waals forces, electrostatic forces, or mechanical forces amongst others; the presence of water or humidity can also be a driving force for agglomerate formation (Hartley et al. 1985; Corn 1961). These forces are particularly effective at binding submicron particles with high surface area to volume ratios (Hartley et al. 1985; Corn 1961).

Nanometer sized fumed silica is a material typically with a primary size of 7- 14 nm (Irfan et al. 2014; Merkel et al. 2002; Raghavan and Khan 1997). It is used as an additive in the manufacturing of products such as thermal insulation panels, sealants, and golf balls. Workers who use or produce fumed silica can be exposed when the raw material is added in the manufacturing process of these items. Exposures to quartz containing crystalline silica are of most concern, however, investigators have also identified potential health effects associated with amorphous, non-crystalline silica. In 1977, Vitums et al. found that workers who had been exposed to fumed silica for an extended period of time had histologically documented pulmonary fibrosis and granulomatous nodules. It has been found that human lung cells exposed to fumed silica resulted in an increase in the presence of reactive oxygen species (ROS) and lactate dehydrogenase (LDH) leakage from the cell membrane (Irfan et al. 2014). Researchers have also observed that exposure to fumed silica in the micron and submicron size range elicited an interleukin 1 $\beta$  (IL-1 $\beta$ ) response (Sandberg et al. 2012; Sun et al. 2016). This response is important because inflammasome

activation has long been considered an important mechanistic pathway for silica induced lung diseases, such as silicosis. These diseases are almost exclusively associated with crystalline silica, but it was found that some types of amorphous silica, fumed silica, can also induce inflammasome activity. The findings of these studies are further corroborated by the work of several other researchers (Kaewamatawong et al. 2005; Zhang et al. 2012).

Real time instruments (RTIs) are important tools for assessing airborne concentrations of particles, nanomaterials recently, and are commonly used for this purpose in both industry and research. Some instruments have used components to pre-separate particles as a way to ensure only the measurable size range enters the instruments. The cyclone has been used as a separator for airborne particles for decades, and it has been hypothesized that the pre-separation unit, i.e. cyclone, of these devices may be a source of instrument measurement variation. Variations in measurements taken by the SMPS nanoscan (TSI 3910), which utilizes a cyclone, and the SMPS (TSI 3936), which does not, have been observed (Yamada et al. 2015). Researchers found that the SMPS nanoscan measured higher concentrations; additionally they observed a larger number of small particles included in the SMPS nanoscan distribution (Yamada et al. 2015). It was hypothesized that this may be due to the cyclone acting as a disperser of weakly agglomerated particles, thus increasing the particle number concentration and decreasing the mean particle size; this study aims to characterize the effect the cyclone may have on RTI measurements. Mechanistically this hypothesis has been confirmed by other researchers. In 1979 Kousaka et al. found that particle agglomerate dispersion can be caused by the acceleration or deceleration of an airstream and obstacles in the airstream; both conditions exist in the cyclone. The RTIs discussed would be used for area monitoring in manufacturing facilities, such as insulation material production. The accuracy of these measurements is important for characterizing true worker

exposures to contaminants in the workplace. Inaccuracies could lead to improper worker protection planning, personal protective equipment decisions, and ultimately workers could be overexposed to hazardous materials.

The purpose of this project was to determine the efficacy and variations of three RTIs in measuring airborne particles generated from an insulation raw material, fumed silica, commonly used across many industries for its low thermal conductivity and thixotropic behavior. The three RTIs used for comparison were the Scanning Mobility Particle Sizer (SMPS) nanoscan, Optical Particle Sizer (OPS), and Fast Mobility Particle Sizer (FMPS). The evaluation was based on analysis of instrument data by each RTI, and particle distribution data collected by a particle sampler, the Tsai Diffusion Sampler (TDS). The SMPS nanoscan and the FMPS were evaluated with and without the cyclone to determine the effects.

## CHAPTER 2: METHODOLOGY

### 2.1 Process

Two generation methods were used to determine the effectiveness of the real time instruments; each method was conducted three times with, and three times without the cyclone. Each experiment lasted forty minutes. The first method, manual pouring, was done by pouring eight grams of fumed silica between two 240 mL natural polypropylene jars; the frequency of pouring was roughly four times per minute and was conducted for ten minutes total. The powder was poured at the brim of the jar, and poured for roughly five seconds each time. However, this was highly operator dependent. The second method, automatic stirring, was done by stirring eight grams of fumed silica inside a 240 mL natural polypropylene jar for ten minutes with an automatic agitator (Model 50006-03, Cole-Palmer) at 400 rpm. During particle generation all RTIs and the particle sampler simultaneously collected data and particles respectively. All experiments were performed inside of a glovebox equipped with an ultra-filter. Experimental setups for stirring and pouring are shown in Fig. 1a and 1b respectively. After each experiment was completed, the glovebox was thoroughly decontaminated and all samplers were removed; RTI data was then collected for ten minutes while no aerosol generation occurred inside the glovebox. The cyclone was not cleaned for this measurement. The experimental process is shown in Fig. 1-2, this figure shows the measurement periods for each experiment.

The OPS, SMPS, and TDS were placed 5 cm away from the rim of the jar, and the FMPS was placed 10 cm away from the jar. The FMPS was placed farther from the location of particle generation because of its significantly higher flow rate (10 L/min) compared to the other instruments and samplers used in the experiment (<1L/min). Grids from the particle sampler were analyzed through TEM analysis.

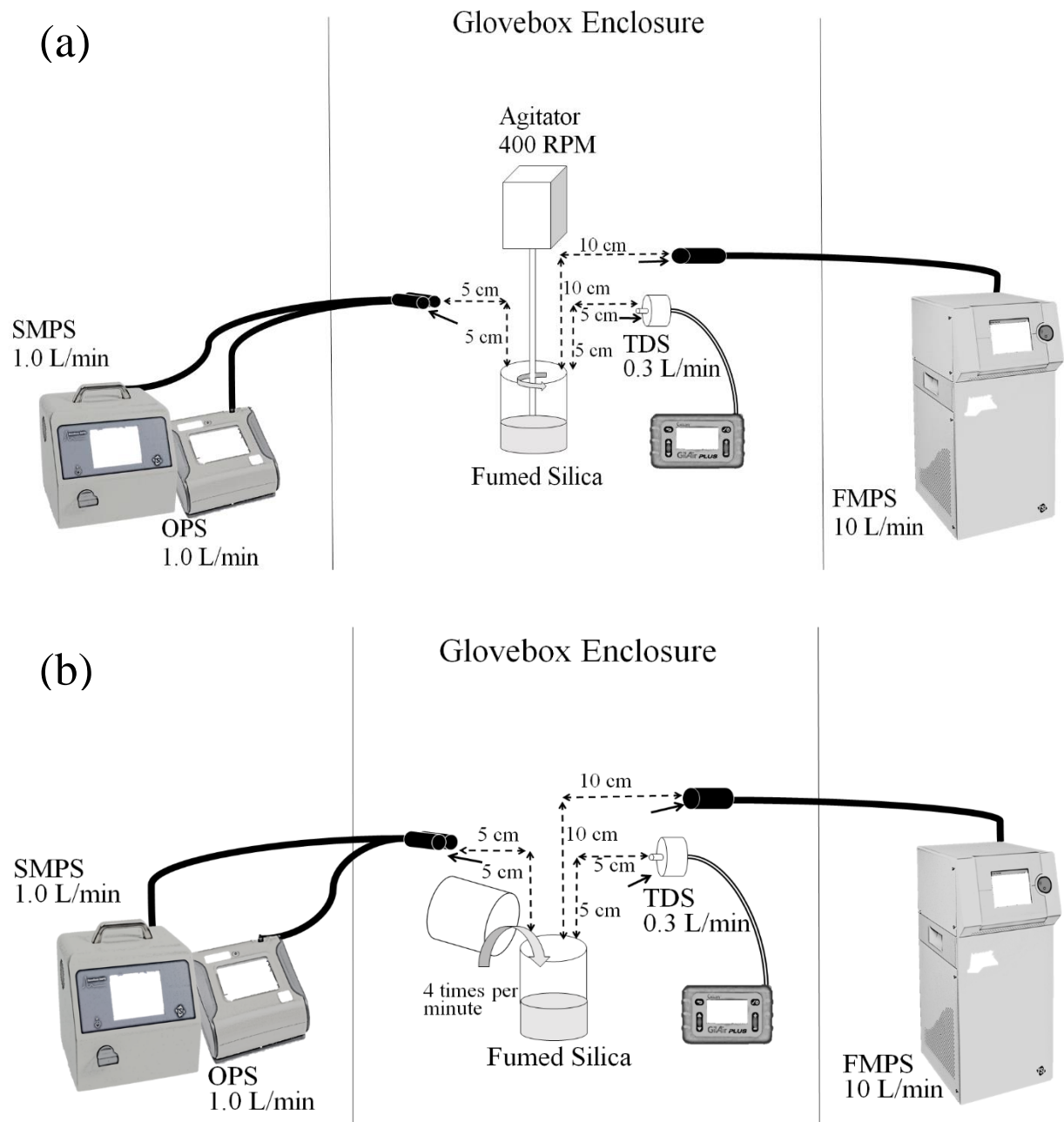


Figure 1-1: Experimental designs for both particle generation methods. a) Experimental design for stirring process, b) Experimental design for pouring process

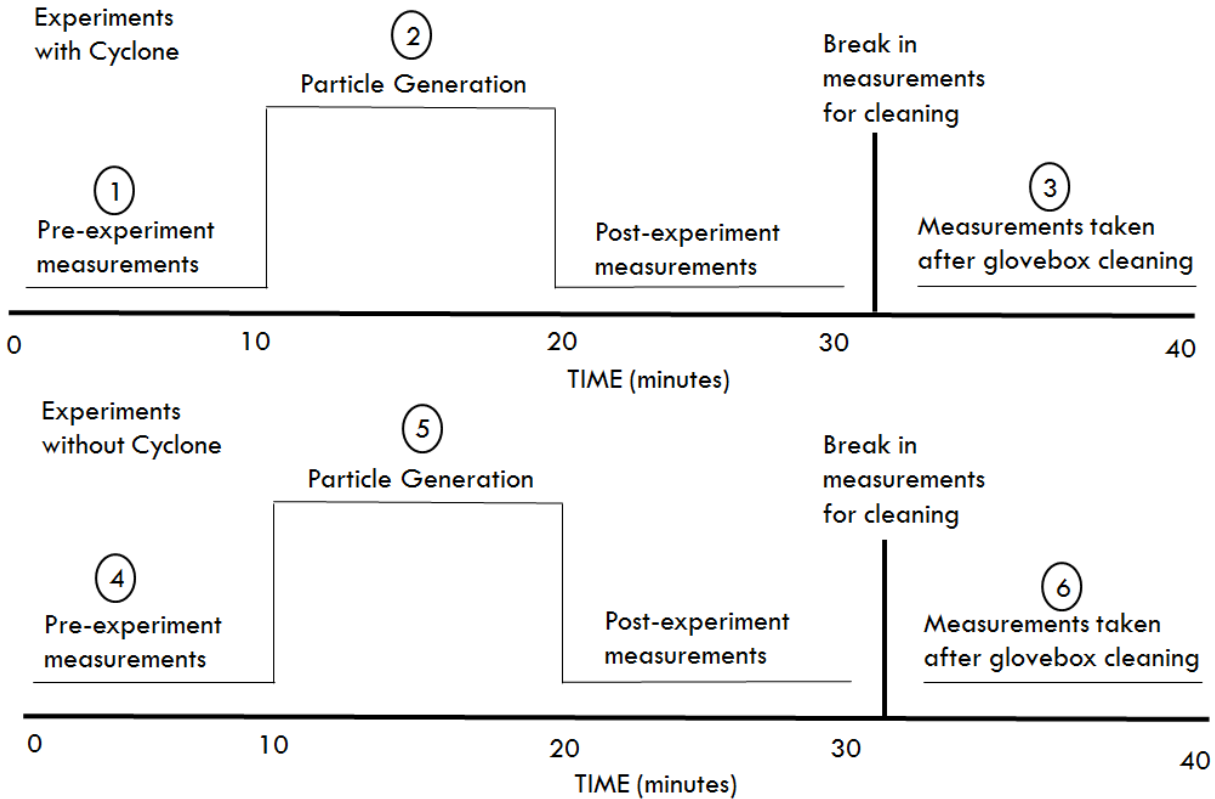


Figure 1-2: Experimental process diagram

## 2.2 Evaluation of Real Time Instrument Measurements

RTIs data were exported from the instrument specific program to Microsoft Excel and analyzed. To demonstrate differences between instruments, four types of graphs were generated from the instrument data. 1) The particle count versus diameter figures were generated using the average particle count for each instrument size channel during pouring or stirring activities. 2) The particle count percentage versus diameter distribution was generated by calculating the percentage of particles measured from each instrument size channel. This distribution was determined to account for size distribution differences between experiments. 3) A total concentration versus time graph was also generated for each experiment and instrument to provide additional information about particle concentration throughout each experiment. 4) A plot of cumulative percentage of particle count versus diameter was used to interpret the combination of aerosols. Most types of

figures displayed data from the experimental time during fumed silica manipulation (stirring, pouring) and from the post-experiment measurements.

### **2.3 Evaluation of Particle Images taken by Electron Microscopy**

Particles collected on grids were analyzed using TEM in order to determine the existence of particles, and morphology of particles for each collected sample. This analysis was performed on a JEOL JEM2100F TEM at 200 kV. Twenty images of grid spaces containing low, medium, and high particle density from each TEM grid were taken. This number of images were collected to ensure images that represented the particle distribution of each sample were obtained. Once images were taken, they were analyzed using FIJI image analysis software (Schindelin et al. 2012). Analysis by this software provided information on the number of particles and their size, allowing researchers to evaluate the distribution of all particles collected. To determine the particle size distribution using FIJI software, a contrast threshold was applied to each image; this eliminated background and allowed for individual particles to be counted. Once the threshold has been applied, FIJI calculated the area of each particle which was then converted to a diameter. Particles were then sorted into 27 size bins and counted. Particles collected on polycarbonate filters were analyzed using a JEOL JSM-6500F scanning electron microscope (SEM) at 15 kV. Twenty images were taken of each sample, and image analysis was conducted with FIJI using the same process described for TEM images.

### **2.4 Statistical Analysis**

A paired t-test was used for each comparison of  $D_{50}$  and particle modes between runs with and without the cyclone and particle generation methods. The  $D_{50}$  represents the median particle diameter measured during each run. In this paper, the  $D_{50}$  has been referred to as the relative  $D_{50}$  because each instrument measures particles in size channels; because the data is separated into size

channels, the actual  $D_{50}$  cannot be determined and the channel that is closest to the cumulative fifty percent of all particles measured was selected. Paired t-tests were also used to compare concentration differences between runs with and without the cyclone. These were used to compare the difference in total concentrations measured after the glovebox was cleaned between runs with and without the cyclone. Additionally, paired t-tests were used to compare the concentrations measured before particle generation and after the glovebox was cleaned between runs with and without the cyclone. P-values obtained from the paired t-test were compared to an alpha level of 0.05. All statistical analysis for this paper was conducted in RStudio, an extension of R.

## **2.5 Materials and Instrumentation**

### **Experimental Media**

Fumed silica (CAS-No.112945-52-5) that contained 90 to 100 percent concentration pyrogenic colloidal silica manufactured by pyrolysis (Sigma-Aldrich, St. Louis, MO) was used for this study. For each experiment eight grams of silica were used.

### **Real Time Instruments**

Aerosol particle assessments were conducted using three RTIs; the SMPS nanoscan (Model 3910, TSI, Shoreview, MN, USA) which measures particle sizes of 10-420 nm in 13 size channels, the OPS (Model 3330, TSI) which measures particle sizes of 0.3 to 10  $\mu\text{m}$  in 16 size channels, and the FMPS (Model 3091, TSI) which measures particles from 5.6 to 560 nm in 32 size channels. The operating principle varies between instruments. The OPS counts particles by measuring the intensity of light refraction created by particles inside the optical chamber. The SMPS counts particles by applying a charge to particles as they enter the instrument and then using isopropyl alcohol, condenses the particles to a size where they can be measured using a spectrometer. The FMPS counts particles by applying a charge to particles as they enter the

instrument, the electrode in the device has a positive charge which repels the particles toward the electrometer, the electrometer then measures particles based upon where they hit on the electrometer. The OPS has a flow rate of 1.0 L/min, the SMPS operates with a flow rate of 0.9 L/min, and the FMPS operates with a flow rate of 10 L/min. The maximum concentrations that can accurately be measured by the OPS, SMPS, and FMPS are 3,000 particles/cm<sup>3</sup>, 1,000,000 particles/cm<sup>3</sup>, and 10,000,000 particles/cm<sup>3</sup> respectively.

### **Particle Sampler**

TDS (Tsai diffusion sampler) collected particles on a silica dioxide filmed, copper transmission electron microscope (TEM) grid and a 25 mm polycarbonate filter with 0.2 μm pores through Brownian motion/diffusion and impaction (for micron particles) in a 25 mm cassette. A Gilian GilAir-3 personal air sampling pump was used at 0.3 L/min.

### **Glovebox**

All experiments were run inside of a glovebox equipped with ultra-filter (manufactured by Terra Universal, Fullerton CA, USA). The dimensions of the glovebox were 35 in. x 24 in. x 25 in. The airflow measured at the sampling location was 2-15 ft./min in the horizontal direction and from 0-6 ft./min in the vertical direction.

## CHAPTER 3: RESULTS AND DISCUSSION

### 3.1 Cyclone Effect during Experimental Process

In this section a comparison of measurements taken during experiments is presented, on Fig. 1-2 this is a comparison of point 2 and 5. The particle concentration and size distributions measured by the RTIs were compared with and without the cyclone attached to the instruments. Data presented in Fig. 1-3 and 1-4 show the average particle counts in each bin range measured by the SMPS and FMPS from both experimental processes with and without the cyclone. No clear trends in particle distribution were observed. However, disparities in total concentration were also observed when the cyclone was used versus when the cyclone was not, and between experimental processes.

Cumulative distributions of particle count versus particle diameter for each particle generation method with and without the cyclone were included in Appendix A; also included was the cumulative distribution functions for each post-experiment. These figures showed the fraction of particles collected in a specific size bin which could be useful for determining the size range and distribution of particles measured by each instrument. The distributions presented in these figures vary significantly, and show no distinct trends.

During the experiments, the majority of particles recorded by the SMPS were between 30 nm and 360 nm in diameter; the majority of particles measured by the FMPS were between 50 nm and 400 nm. These ranges were relatively consistent amongst all runs. However, the modes of measurements taken by the SMPS and FMPS did change between experiments with and without the cyclone. The modes for the SMPS measurements during experiments where the cyclone was used and not used were 170nm and 160 nm respectively. The modes for the FMPS measurements during experiments where the cyclone was used and not used ranged between 140 nm and 160 nm.

However, neither difference was statistically significant as the p-values were 0.80 and 0.34 for the SMPS and FMPS comparison respectively.

### **3.2 Effect of Particle Generation Method**

In this paper the effect of particle generation methods on particle distribution was investigated. Differences in the distribution of particles were observed between stirring and pouring experiments. However none of the observed differences had statistical significance. The  $D_{50}$  of particles measured by the SMPS during stirring and pouring activities when the cyclone was used were 116 nm and 154 nm respectively (p-value: 0.67). When the cyclone was not used the relative  $D_{50}$  was exactly opposite, with 154 nm during stirring activities and 116 nm during pouring activities (p-value: 0.29). The  $D_{50}$  of particles measured by the FMPS during stirring and pouring activities when the cyclone was used were 124 nm and 143 nm respectively (p-value: 0.42). When the cyclone was not used the relative  $D_{50}$  was 143 nm for both stirring pouring activities (p-value: 0.42). None of the observed differences in  $D_{50}$  were statistically significant, indicating the particle generation methods did not affect the particle size of the generated aerosol.

### **3.3 Post-cleaning Concentration and Distribution Results**

In this section a comparison of points 3 and 6 on Fig. 1-2 is presented. After the experiments were run and the glovebox was cleaned, the majority of particles recorded by the SMPS and FMPS were between 20 nm to 275 nm and 50 nm to 300 nm respectively. The average mode particle size measured by the SMPS after the glovebox did not vary significantly between experiments where the cyclone was used and not used; these modes were around 55 nm (p-value: 0.74). The average mode particle size measured by the FMPS did significantly vary between experiments where the cyclone was used and not used. The mode particle size measured by the FMPS after cleaning the glovebox was 52 nm and 8.0 nm when the cyclone was used and not used

(p-value: 0.004). In addition to mode particle size, the  $D_{50}$  is also useful for determining the measured particle distribution. After cleaning the glovebox, the relative  $D_{50}$  measured by the SMPS during stirring experiments with and without the cyclone were 49 nm and 65 nm respectively; there was not a statistically significant difference between these values (p-value: 0.80). For pouring experiments these values were 37 nm for both runs with and without the cyclone (p-value: 0.75). For the FMPS, after the glovebox was cleaned, the relative  $D_{50}$  measured during stirring experiments with and without the cyclone were 52 nm and 34 nm respectively (p-value: 0.65). For pouring experiments these values were 93 nm and 22 nm with and without the cyclone (p-value: 0.01). This measurement in addition to the difference in mode particle size measured by the FMPS were the only statistically significant findings pertaining to particle size differences after the glovebox was cleaned. The significant decrease in median and mode particle size measured by the FMPS when the cyclone was not used was unexpected as it deviates from the hypothesis that the cyclone would break agglomerated particles into smaller particles.

As shown in Table 1, the FMPS and SMPS recorded greater concentrations after each experiment and glovebox cleaning when the cyclone was used than after experiments where the cyclone was not used. When the cyclone was used, during the no aerosol generation period after stirring and pouring experiments the average SMPS concentration recorded in the glovebox was  $1.3 \times 10^3$  particles/cm<sup>3</sup> and  $1.2 \times 10^3$  particles/cm<sup>3</sup> respectively. When the cyclone was not used, the SMPS recorded 51 particles/cm<sup>3</sup> and 110 particles/cm<sup>3</sup> during the no aerosol generation period after stirring and pouring respectively. Likewise, when the cyclone was used the FMPS recorded  $1.1 \times 10^4$  particles/cm<sup>3</sup> and  $2.5 \times 10^4$  particles/cm<sup>3</sup> during the no aerosol generation period after stirring and pouring respectively; when the cyclone was not used the FMPS recorded 500 particles/cm<sup>3</sup> and 860 particles/cm<sup>3</sup> during the no aerosol generation period after stirring and

pouring respectively. This indicated contamination from the cyclone had an effect on the particle concentrations measured by the SMPS and FMPS as residual particles trapped in the cyclone from particle generation were likely being dispersed from within the cyclone unit. Standard deviations from the average concentration of all three runs per experiment type are included in Table 1-1. It must be noted that the standard deviations are relatively large; this can be attributed to the inconsistencies in the particle generation process. A huge amount of variability was present in these processes as they require periodic human intervention to continuously generate particles. Average particle concentrations over time are also presented in Appendix B. These figures show the how variable the concentration was throughout each experiment.

To test the significance and accuracy of this finding, a paired t-test between runs with and without the cyclone for each data set was conducted; this data is summarized in Table 1-2. Using a significance value of 0.05, it was found that all runs within each data set with and without cyclone use were statistically different from each other. In addition, almost all runs with the cyclone had higher particle counts compared to runs without the cyclone. This corroborates the hypothesis that the cyclone breaks large particle agglomerates into smaller particles and therefore causes a measureable increase in particle concentration measurements. However, during the second run of stirring experiments when the cyclone was not used the FMPS measured higher particle concentrations than when the cyclone was used; this observation was also seen during the second run of pouring experiments when the SMPS recorded higher particle concentrations when the cyclone was not used than when cyclone was used. These results indicate the process is highly dependent on how the operator handled the sample during particle generation. This is representative of how materials would be handled in the work environment.

All OPS runs, with the exception of the second set of stirring experiments, were also statistically different ( $p < 0.05$ ) from each other. This outcome is expected as consistent differences in particle counts at low concentration will still yield statistically significant differences. The effect of the cyclone is shown in the mean particle count differences of each instrument. The SMPS and FMPS usually had higher particle counts when the cyclone was used (except for one FMPS stirring comparison), and the difference in particle counts ranged from 60 to  $3.5 \times 10^3$  particles/cm<sup>3</sup> for the SMPS and 90 to  $4.8 \times 10^4$  particles/cm<sup>3</sup> for FMPS. The OPS recorded higher particle counts for three out of six comparisons where the FMPS and SMPS did not have the cyclone attached, and the mean difference in particle counts ranged from 0.5 to 3.4 particles/cm<sup>3</sup>. Although every run was statistically different from its paired equivalent, the large discrepancy in mean particle count differences between the OPS and the other instruments provided further evidence that the cyclone may have contributed to particle counts.

Table 1-1: Average Total Particle Number Concentration for All Runs

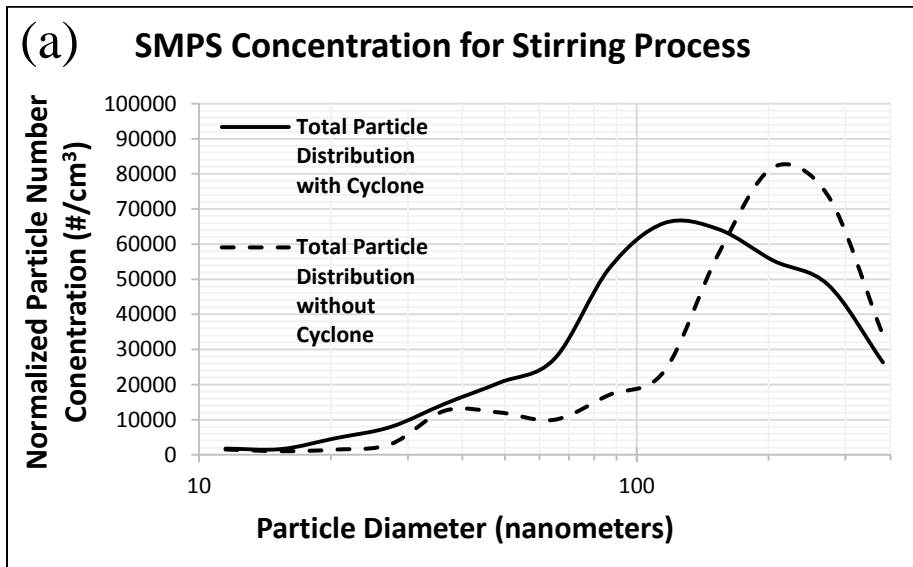
Experimental Process	Presence of Cyclone (On SMPS and FMPS)	Total Concentration (#/cm <sup>3</sup> )		
		OPS	SMPS	FMPS
Stirring	Cyclone	210(±46)	5,000(±7,400)	43,000(±8,300)
	No Cyclone	750(±400)	40,000(±18,000)	170,000(±100,000)
Pouring	Cyclone	360(±290)	28,000(± 32,000)	100,000(±110,000)
	No Cyclone	620(±280)	4,900(±1,500)	67,000(±34,000)
Post-Expt Stirring	Cyclone	1.1(±1.6)	1,300 (±2,000)	11,000(±10,000)
	No Cyclone	0.9(±0.4)	51(±61)	500(±290)
Post-Expt Pouring	Cyclone	0.6(±0.7)	1,200(±1,800)	25,000(±21,000)
	No Cyclone	0.2(±0.1)	110(±75)	860(±390)

Note: Average total concentration of three data sets measured by each instrument during the identified experimental process. The size range measured by each instrument were as follows (1) OPS: 300-10,000 nm (2) SMPS: 10-420 nm (3) FMPS: 5-560 nm.

Table 1-2: Paired t-test results between runs with and without cyclone after glovebox cleaning

Experimental Data Set	OPS		SMPS		FMPS	
	p-value	Mean conc differ (#/cm <sup>3</sup> )	p-value	Mean conc differ (#/cm <sup>3</sup> )	p-value	Mean conc differ (#/cm <sup>3</sup> )
Stirring Set 1	3.1 x 10 <sup>-10</sup>	-0.51	6.3 x 10 <sup>-14</sup>	3,532	< 2.2 x 10 <sup>-16</sup>	10,985
Stirring Set 2	6.3 x 10 <sup>-02</sup>	-1.14	1.1 x 10 <sup>-08</sup>	99	< 2.2 x 10 <sup>-16</sup>	-94
Stirring Set 3	4.9 x 10 <sup>-13</sup>	2.30	4.9 x 10 <sup>-04</sup>	60	< 2.2 x 10 <sup>-16</sup>	20,046
Pouring Set 1	8.4 x 10 <sup>-04</sup>	0.074	8.7 x 10 <sup>-12</sup>	3,249	< 2.2 x 10 <sup>-16</sup>	21,199
Pouring Set 2	< 2.2 x 10 <sup>-16</sup>	-3.45	2.3 x 10 <sup>-12</sup>	-164	< 2.2 x 10 <sup>-16</sup>	4,618
Pouring Set 3	1.8 x 10 <sup>-08</sup>	1.13	1.0 x 10 <sup>-06</sup>	175	< 2.2 x 10 <sup>-16</sup>	47,676

Note: These values were generated from a paired t-test between runs with and without the cyclone after the glovebox was cleaned. The difference in mean particle counts represents the difference compared to the run without the cyclone. Positive values indicate the run with the cyclone had more particles counted, while negative values indicate the run without the cyclone had more particles counted. The t-test was run in R.



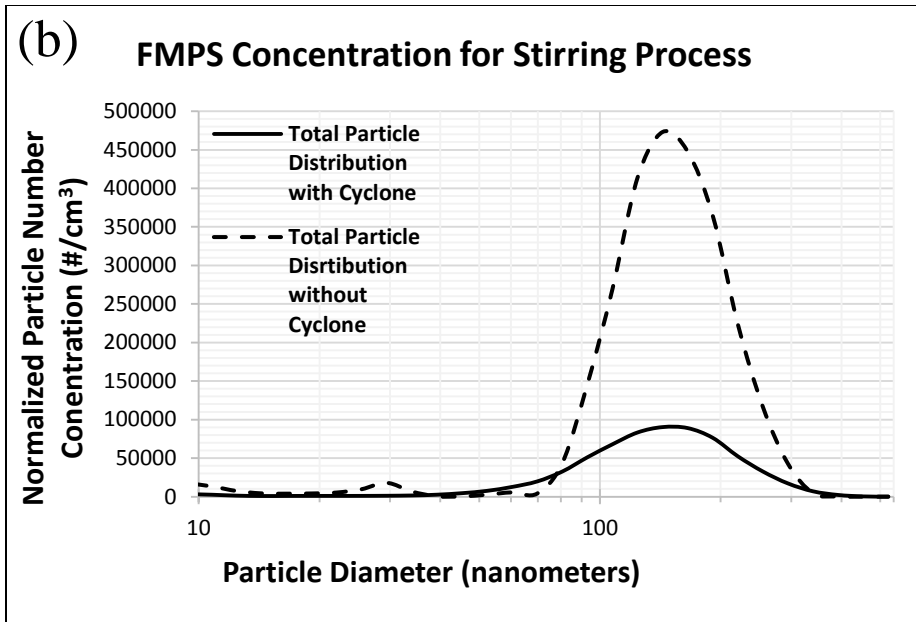
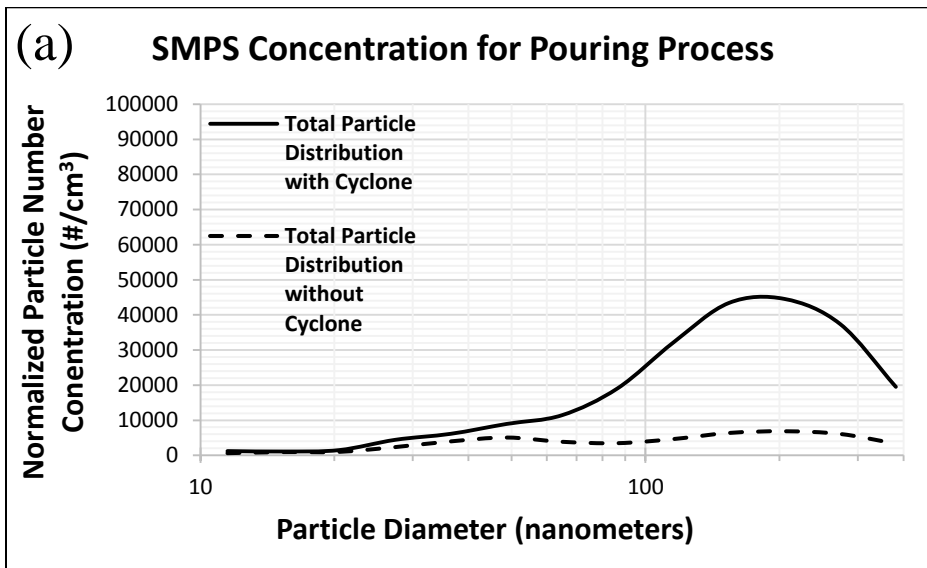


Figure 1-3: Average particle count measured by the RTIs during all stirring process runs. a) Average SMPS particle count during all stirring process runs, b) Average FMPS particle count during all stirring process runs

Note: Size range measured by FMPS is 5 nm to 560 nm, and size range measured by SMPS is 10 nm to 420 nm.



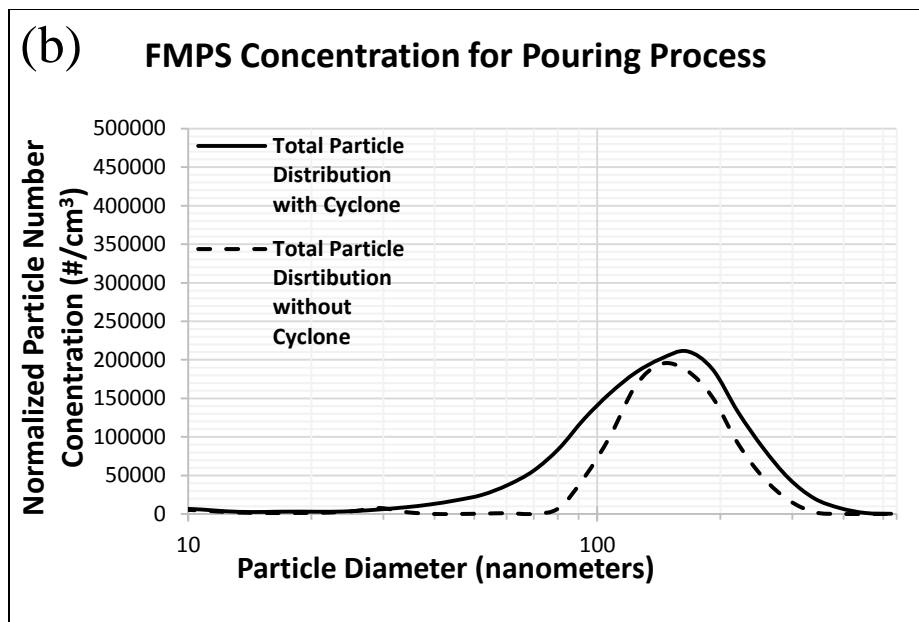


Figure 1-4: Average particle count measured by the RTIs during all pouring process runs. a) Average SMPS particle count during all stirring process runs, b) Average FMPS particle count during all stirring process runs

Note: Size range measured by FMPS is 5 nm to 560 nm, and size range measured by SMPS is 10 nm to 420 nm.

### 3.4 Comparison of Pre-Experiment and Post-Cleaning Concentrations

In this section a comparison of the concentration measurements taken before particle generation and after the glovebox was cleaned was presented. This was a comparison of points 1 and 3, and 4 and 6 on Fig. 1-2. The data presented in this section show the differences in concentrations measured in the clean glovebox before and after each experiment. This allows for a comparison of RTI measurements taken with a clean cyclone and a contaminated cyclone in the clean glovebox. In runs where the cyclone was used, the cyclone was cleaned prior to particle generation but not before the glovebox was decontaminated. Measurements taken when the cyclone was used and when the cyclone was not used were also compared. During stirring runs when the cyclone was used, the SMPS and FMPS measured an average of 1,150 and 10,600 more particles/cm<sup>3</sup> respectively after the glovebox was cleaned, when the cyclone was contaminated, than before particle generation, when the cyclone was clean. During pouring runs when the cyclone

was used, the SMPS and FMPS measured an average of 1,060 and 24,900 more particles/cm<sup>3</sup> respectively after the glovebox was cleaned than before particle generation. During stirring experiments when the cyclone was not used, the SMPS and FMPS measured an average of 88 and 12 fewer particles/cm<sup>3</sup> respectively after the glovebox was cleaned than before particle generation. During pouring experiments when the cyclone was not used, the SMPS and FMPS measured an average of 50 and 714 more particles/cm<sup>3</sup> respectively after the glovebox was cleaned than before particle generation. When comparing experiments with and without the cyclone, the number of particles measured before particle generation and after the glovebox cleaning was significantly larger when the cyclone was used than when the cyclone was not used. This comparison provided further evidence that residual particles trapped in the cyclone were contributing to concentration measurements. Greater average concentrations during the measurement period before particle generation were only observed during pouring experiments when the cyclone was not used.

### **3.5 TEM and SEM Size Distribution Analysis**

The TDS collects particles on a polycarbonate filter and a TEM grid. The pore size of the filter used was 200 nm, this allows for larger particles to mostly be impacted on to the filter, while smaller particles are primarily deposited onto the TEM grid due to Brownian motion. The use of the TEM grid and filter together allowed for a wide range of particles to be collected and analyzed. Images of particles collected on the TEM grids using the TDS were shown in Fig. 1-5a through 1-5d. An overview image at low magnification showed the distribution of particles collected on the grid spaces. The image of a single grid space, also shown in Fig. 1-5, was shown to provide an example of fume silica particles at various sizes.

The majority of particles collected by the particle sampler were in the size range of 12 nm to 337 nm with the D<sub>50</sub> and mean particle diameter collected on the TEM grid being 115.5 nm.

This range is comparable to the range of particle collected by the SMPS and FMPS which measured particles from 20 nm to 300 nm. In addition, the median particle diameter measured by the SMPS during stirring with the cyclone and during pouring without the cyclone was identical to the median particle diameter collected on the TEM grid.

SEM images of particles collected by the TDS onto the filters are shown in Fig. 1-5c and 1-5d. It was found that TDS collected filter particles in the range of 11.5 nm to 16  $\mu\text{m}$ , with the majority of particles between 400 nm and 9  $\mu\text{m}$ . The mean particle diameter collected on the filters was 2,800 nm, and the  $D_{50}$  was 1,300 nm. Data from the RTIs did not include very many particles above 400 nm. The presence of these particles on the particle sampler filter indicated that the RTIs may underestimate the presence of larger particles, which may have been caused by deagglomeration in the cyclone.

This data further verifies the measurements taken by the RTIs as the  $D_{50}$  of particles collected on the TEM grids was similar to the  $D_{50}$  of particles measured by the SMPS and FMPS. Additionally the primary measurement range of the RTIs is similar to the size range of particles collected on the TEM grid of the particle sampler. However, the SEM images of the filters showed that the measurement by the RTIs above 400 nm underestimated particle concentration due to minimal particle counts.

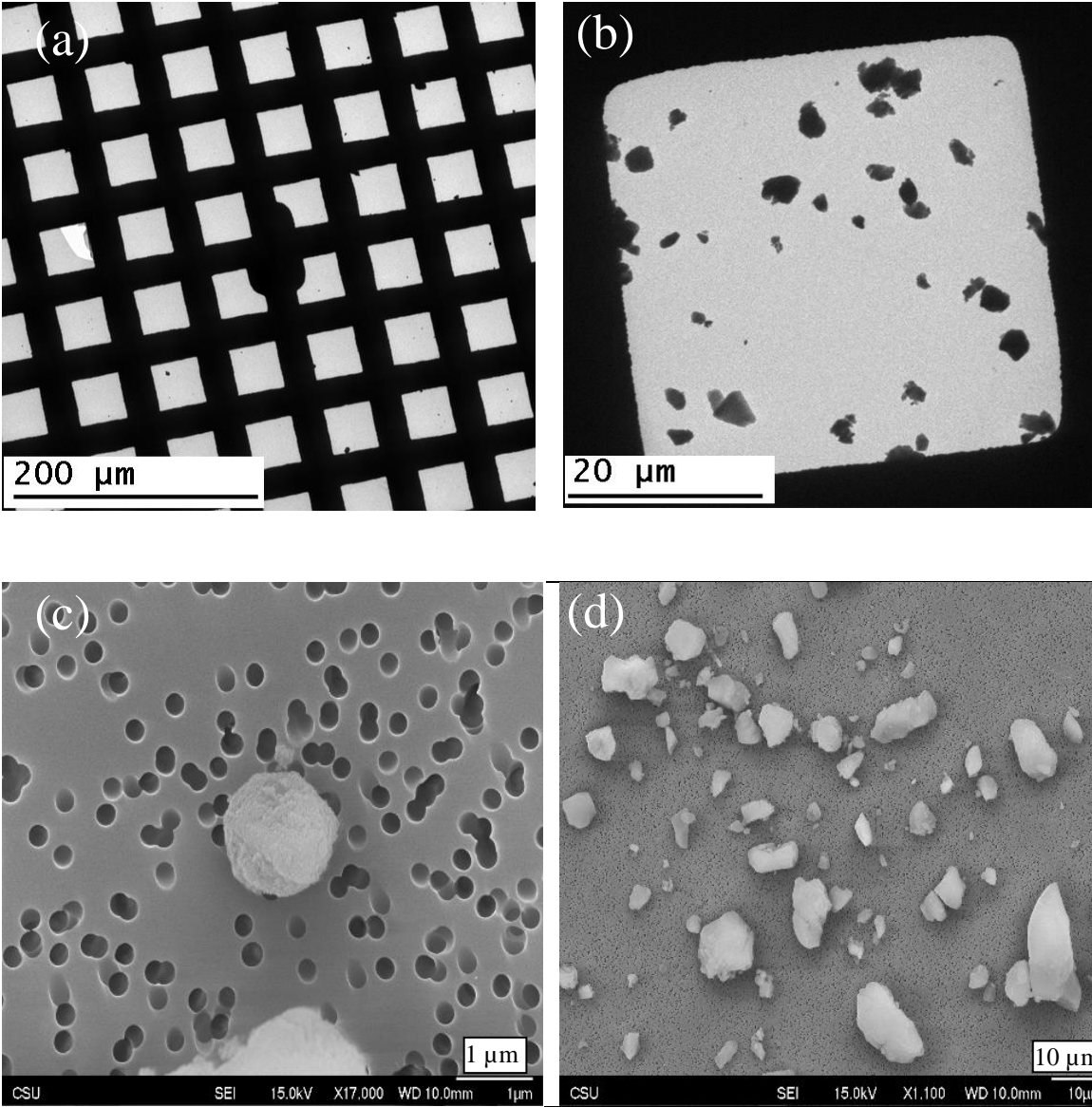


Figure 1- 5: Electron microscopy images. a) TEM image overview of grid containing fumed silica particles on silica dioxide film of grid space, b) TEM images of fumed silica particles on silica dioxide film of one grid space, c) SEM images of fumed silica on polycarbonate filter at high magnification view (x17,000) and d) SEM images of fumed silica on polycarbonate filter at low magnification view (x1,100)

## CHAPTER 4: CONCLUSION

RTIs that use a pre-separation unit, or cyclone, were compared to determine the effects of the cyclone. Statistically significant differences in concentration were observed after the glovebox was cleaned between experimental runs where the cyclone was used and runs where the cyclone was not used. When the cyclone was used, the measured concentrations were much greater than when the cyclone was not used. Because the glovebox was clean, it could reasonably be concluded that the measured concentrations during runs where the cyclone was used could be attributed to residual particles trapped in the cyclone. No significant differences between the distributions of particles generated during stirring and pouring experiments were observed.

Based upon the data presented, it was found that the cyclone greatly affected the measurements taken by the RTIs, with the greatest differences in concentration measurements being observed in cleaner environments. While it seemed as though the cyclone was one of the primary contributing factors to instrument measurement variation, it should not be removed as it played an important role in removing larger particles from the sampling train of the RTIs. This is critical function because particles above the measurement range of the instrument will not be accurately sized and could potentially bias the instrument measurements. Additionally, large particles entering the instrument could also block the sampling train entirely. Because of this, it is recommended that the cyclone be cleaned after each use to ensure the highest level of accuracy in RTIs measurements.

## REFERENCES

- Corn, M. (1961). The Adhesion of Solid Particles to Solid Surfaces, I. a Review, *Journal of the Air Pollution Control Association*, 11(11):523-528.
- Hartley, P. A., Parfitt, G. D., Pollack, L. B. (1985). The role of the van der Waals force in the agglomeration of powders containing submicron particles, *Powder Technology*, 42(1) 35-46.
- Irfan, A., Cauchi, M., Edmands, W., Gooderham, N., Njuguna, J., Zhu, H. (2014). Assessment of Temporal Dose-Toxicity Relationship of Fumed Silica Nanoparticle in Human Lung A549 Cells by Conventional Cytotoxicity and H-NMR-Based Extracellular Metabonomic Assays, *Toxicological Sciences*, Oxford, United Kingdom, 138(2):354-364.
- Kaewamatawong, T., Kawamura, N., Okajima, M., Sawada, M., Morita, T., Shimada, A. (2005). Acute Pulmonary Toxicity Caused by Exposure to Colloidal Silica: Particle Size Dependent Pathological Changes in Mice, *Toxicology Pathology*, 33(7):745-751.
- Kousaka, Y., Okuamama, K., Shimizu, A., Yoshida, T. (1979). Dispersion Mechanism of Aggregate Particles in Air, *Journal of Chemical Engineering of Japan*, 12(2):152-159.
- Merkel, T. C., Freeman, B. D., Spontak, R. J., He, Z., Pinnau, I., Meakin, P., Hill, A. J. (2002). Ultraporous, Reverse-Selective Nanocomposite Membranes, *Science*, 296(5567):519-522.
- Raghavan, S. and Khan, S. (1997). Shear-Thickening Response of Fumed Silica Suspensions under Steady and Oscillatory Shear, 185(1):57-67.
- Sandberg, W., Lag, M., Holme, J., Friede, B., Maurizio, G., Kruszewski, M., Schwarze, P., Skuland, T., Refsnes, M., author, E. (2012). Comparison of non-crystalline silica nanoparticles in IL-1 $\beta$  release from macrophages, *Particle and Fibre Toxicology*, 9(32):1-13.
- Schindelin, J., Arganda-Carreras, I., Frise, E., Kaynig, V., Longair, M., Pietzsch, T., Preibisch, S., Rueden, C., Saalfeld, S., Schmid, B. (2012). Fiji: an open-source platform for biological-image analysis. *Nature methods*, 9:676-682.
- Sun, B., Wang, X., Liao, Y.-P., Ji, Z., Chang, C. H., Pokhrel, S., Ku, J., Liu, X., Wang, M., Dunphy, D. R., Li, R., Meng, H., Madler, L., Brinker, J., Nel, A. e. E., Xia, T. (2016). Repetitive Dosing of Fumed Silica Leads to Profibrogenic Effects through Unique Structure–Activity Relationships and Biopersistence in the Lung, *ACS Nano*, 10(8):8054–8066.
- Vitums, V. C., Edwards, M. J., Niles, N. R., Borman, J. O., Lowry, R. D. (1977). Pulmonary Fibrosis from Amorphous Silica Dust, A Product of Silica Vapor, *Archives of Environmental and Occupational Health*, 32(2):62-68.
- Yamada, M., Takaya, M., Ogura, I. (2015). Performance evaluation of newly developed portable aerosol sizers used for nanomaterial aerosol measurements, *Industrial Health*, 53(6):511-516.
- Zhang, H., Dunphy, D. R., Jiang, X., Meng, H., Sun, B., Tarn, D., Xue, M., Wang, X., Lin, S., Ji, Z., Li, R., Garcia, F. L., Yang, J., Kirk, M. L., Xia, T., Zink, J. I., Nel, A., Brinker, C. J. (2012). Processing pathway dependence of amorphous silica nanoparticle toxicity: colloidal versus pyrolytic, *Journal of the American Chemical Society*, 134(38):15790–15804.

APPENDIX A

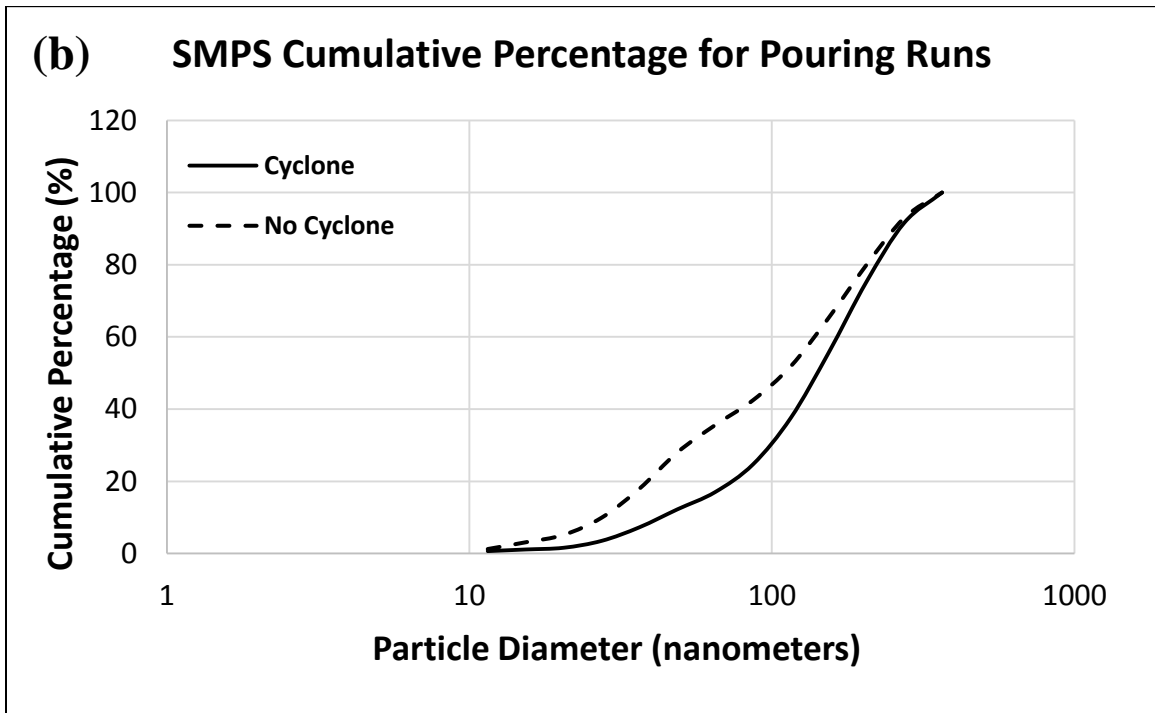
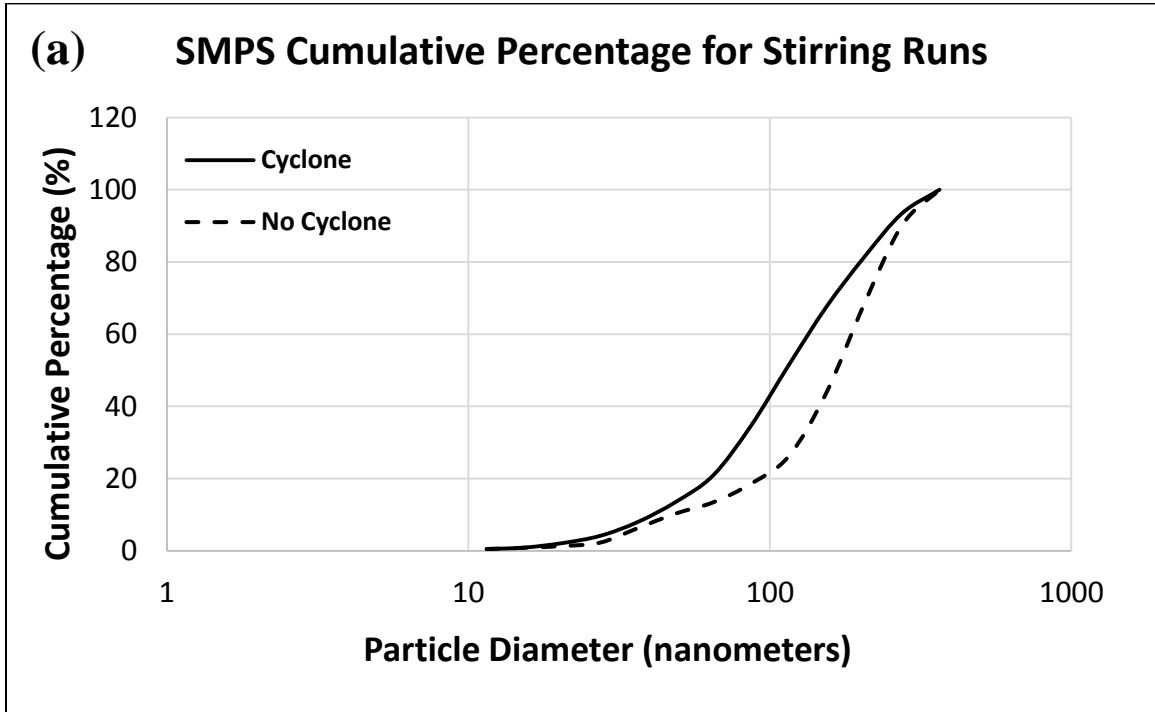


Figure 1-S1: Average particle cumulative percentage measured by the SMPS for all experimental runs: (a) cumulative percentage for stirring runs, (b) cumulative percentage for pouring runs

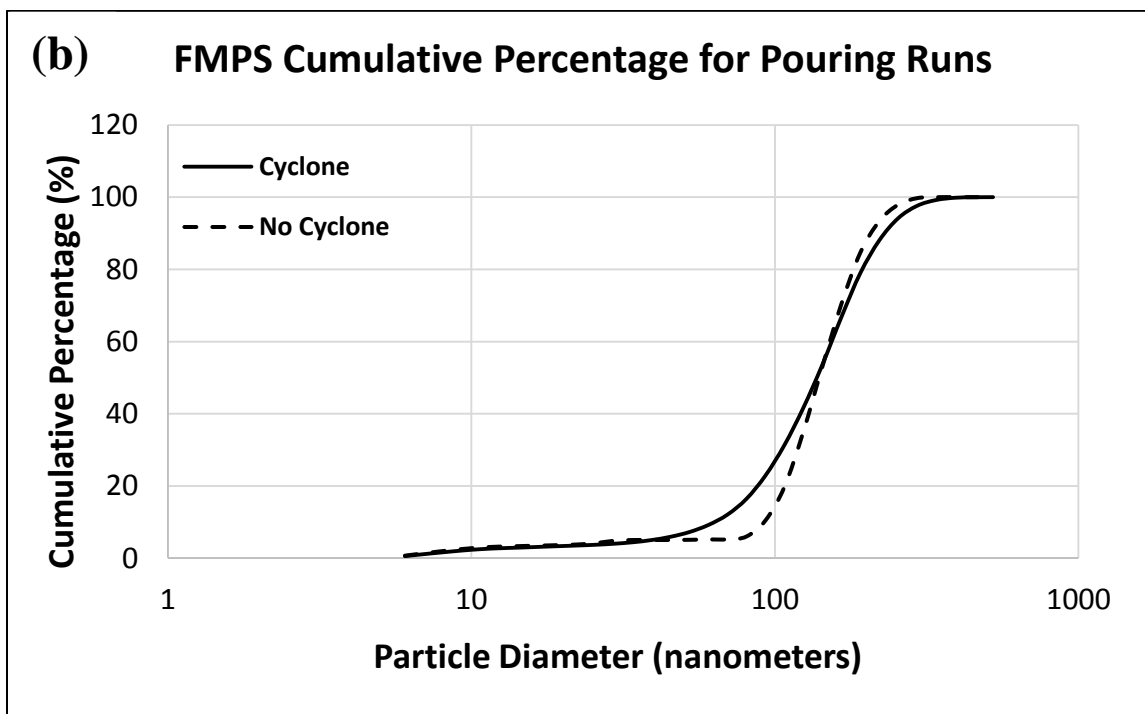
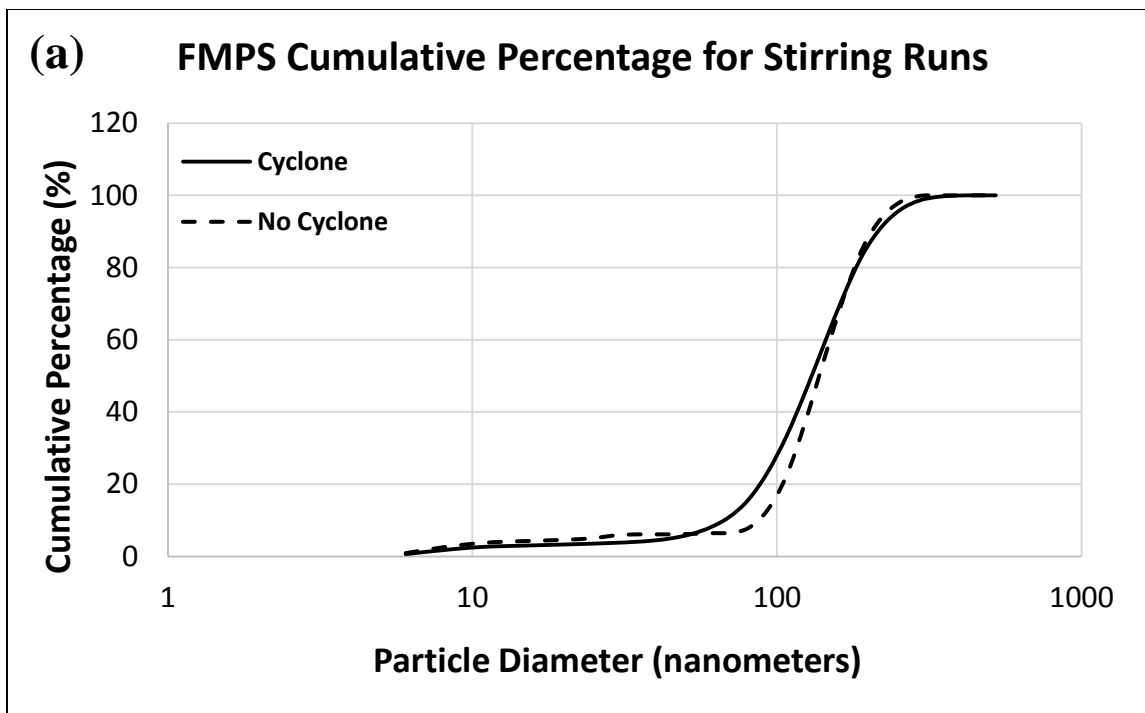


Figure 1-S2: Average particle cumulative percentage measured by the FMPS for all experimental runs: (a) cumulative percentage for stirring runs, (b) cumulative percentage for pouring runs

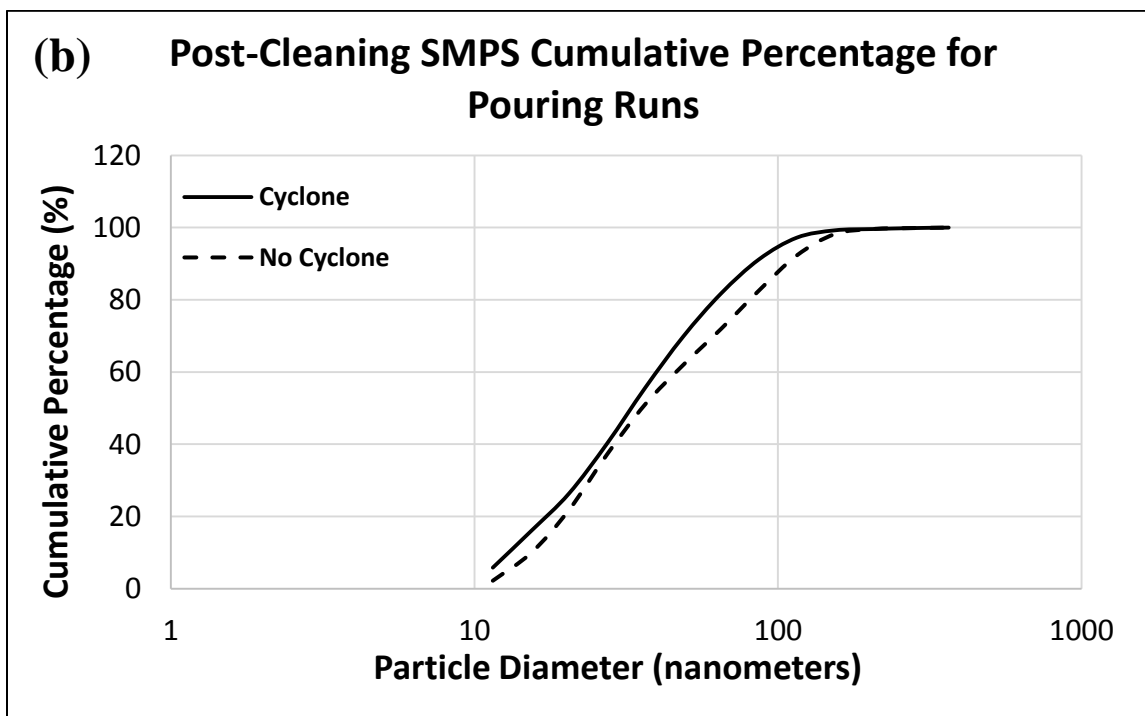
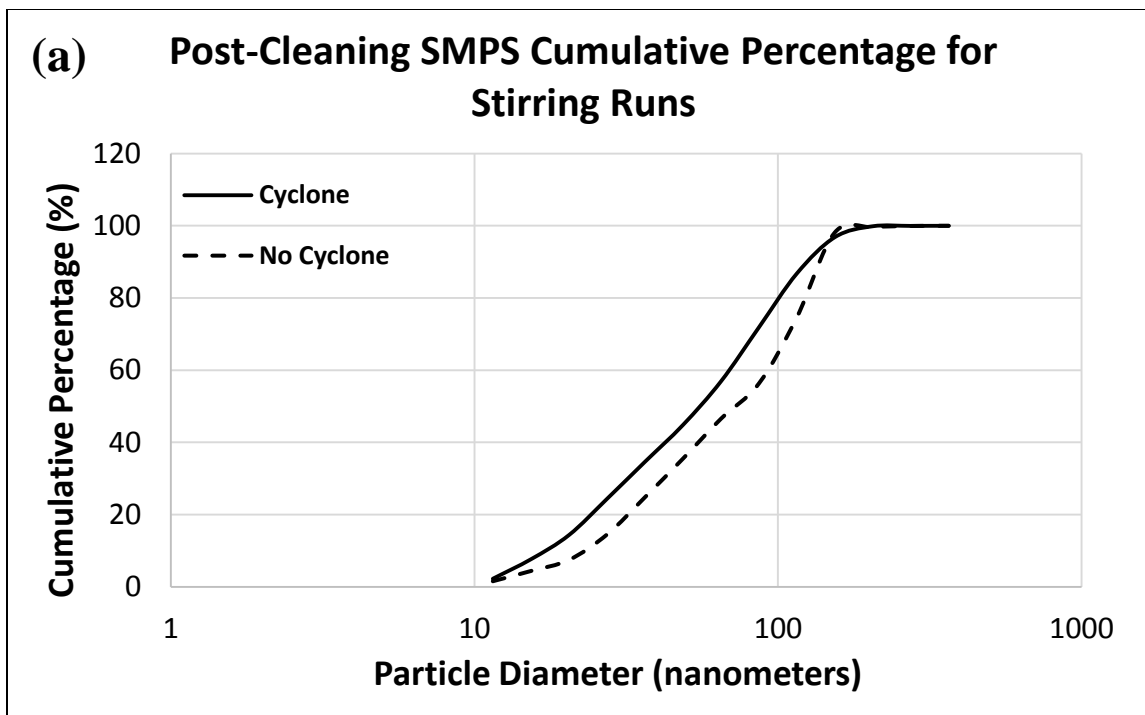


Figure 1-S3: Average particle cumulative percentage measured by the SMPS after the glovebox was cleaned for all runs (a) cumulative percentage for particles measured after stirring runs, (b) cumulative percentage for particles measured after pouring runs

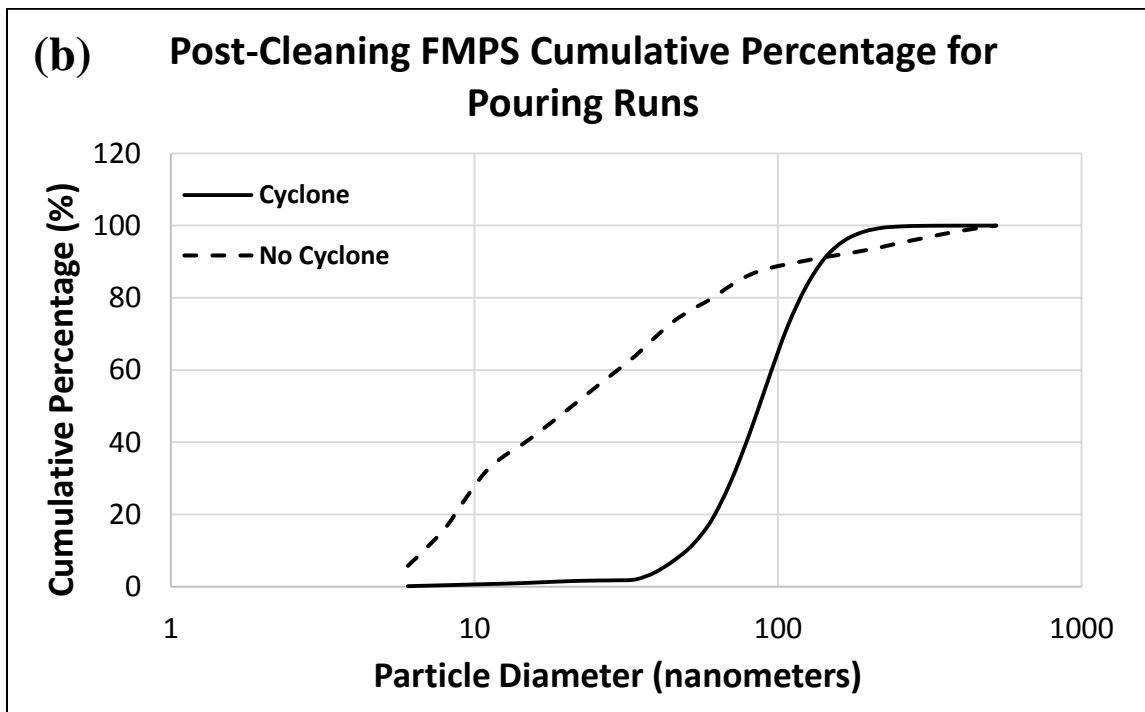
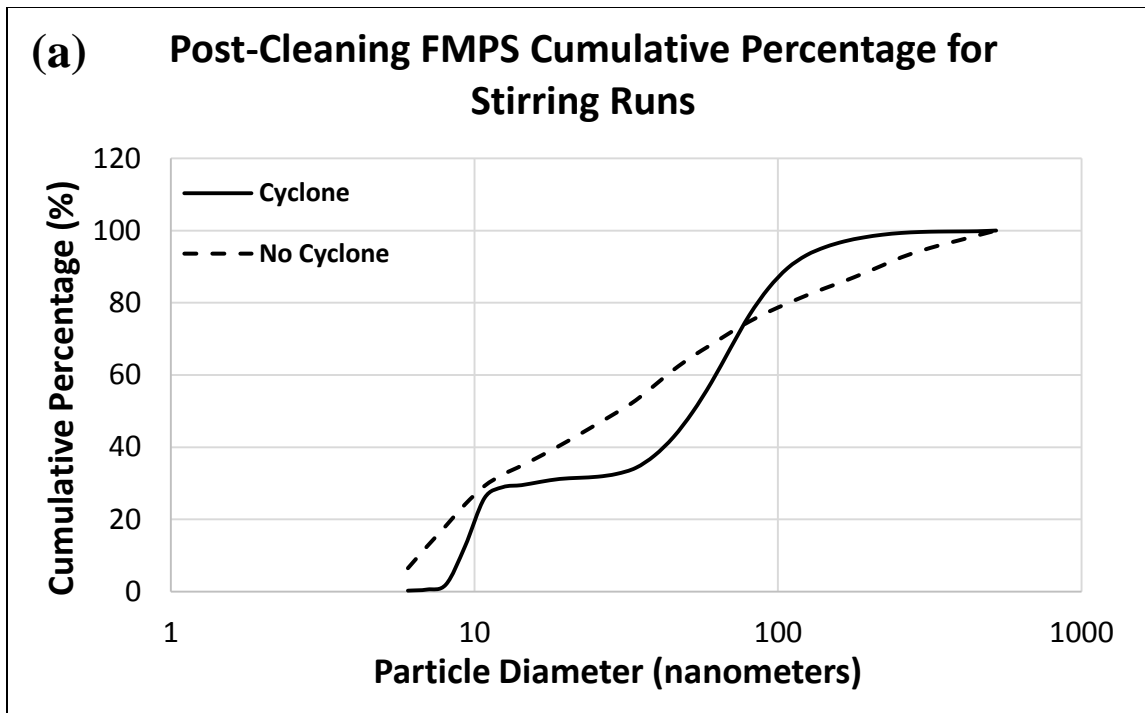


Figure 1-S4: Average particle cumulative percentage measured by the FMPS after the glovebox was cleaned for all runs (a) cumulative percentage for particles measured after stirring runs, (b) cumulative percentage for particles measured after pouring runs

## APPENDIX B

### SMPS

### FMPS

### OPS

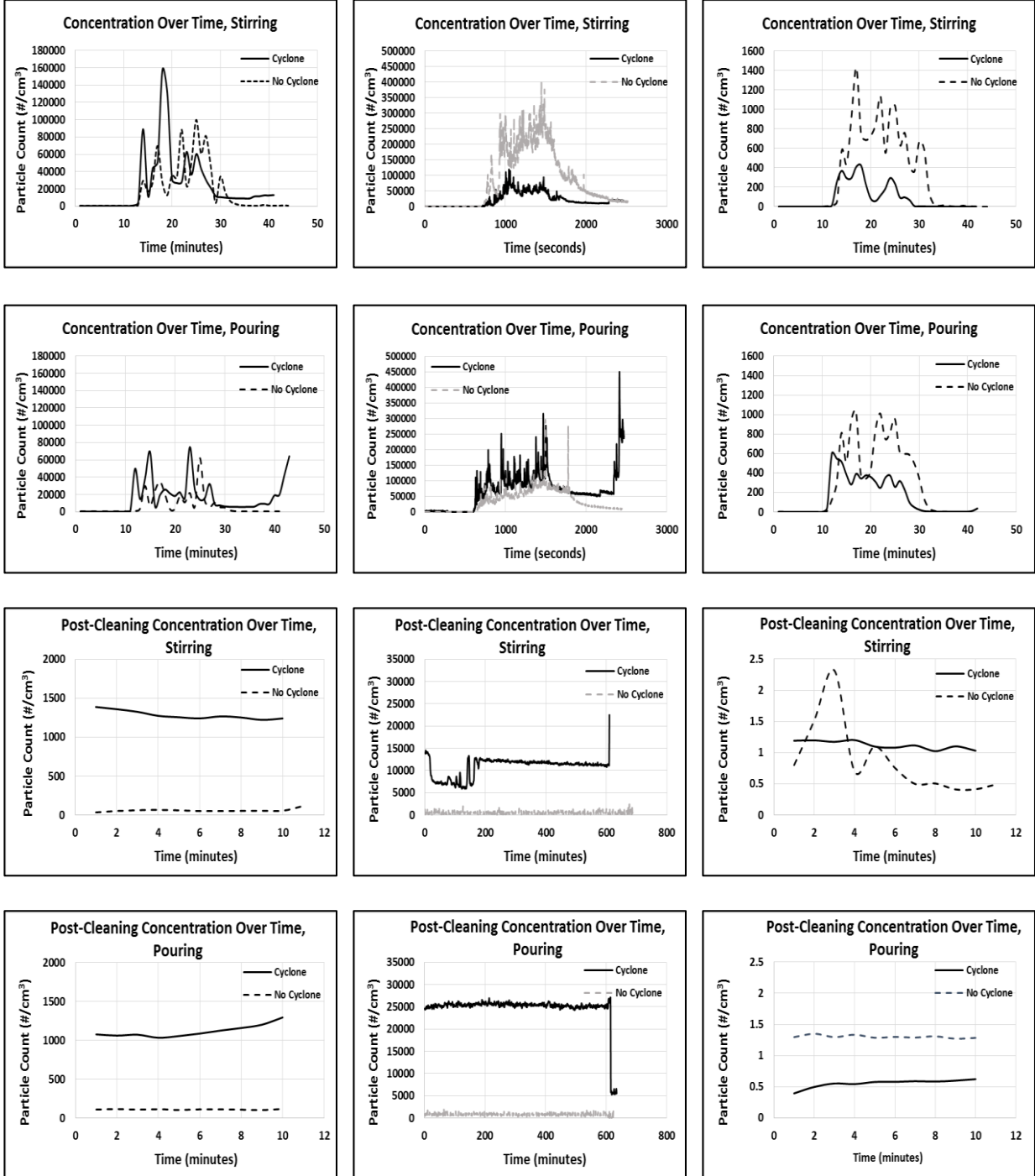


Figure 1-S5: Average Concentration over Time for all experiments

## LIST OF ACRONYMS

FMPS.....	Fast Mobility Particle Sizer
LDH.....	Lactate Dehydrogenase
OPS.....	Optical Particle Sizer
ROS.....	Reactive Oxygen Species
RTL.....	Real Time Instrument
SEM.....	Scanning Electron Microscope
SMPS.....	Scanning Mobility Particle Sizer
TEM.....	Transmission Electron Microscope
TDS.....	Tsai Diffusion Sampler

PART TWO:

A COMPARISON OF NIOSH 7402 AND THE TSAI DIFFUSION SAMPLER FOR  
COLLECTING AND ANALYZING CARBON NANOTUBES

## CHAPTER 1: INTRODUCTION

Carbon nanotubes (CNTs) were first synthesized by Japanese physicist Sumio Iijima in 1991. Since their inception, CNTs have been increasingly utilized in many industries because of the material's exceptional thermal and electrical conductivity in addition to their strength (Bateson et al. 2017). In recent years, CNT exposure has been of increasing concern because of their morphological similarities to asbestos (Donaldson et al. 2006). CNT toxicity has been demonstrated in a number of animal studies, which suggest they may have significant impact on pulmonary cells by inducing inflammation, granulomas, and fibrotic reactions (Muller et al. 2005; Lam et al. 2004; Poland et al. 2008).

CNTs are respirable particles with individual fibers having been observed to be 4-100 nm in diameter and 50 nm to 15 $\mu$ m in length (Bateson et al. 2017; Iijima 1991; Wang et al. 2009; Yamashita et al. 2010). Because of their small size and ability to elicit a pathological response similar to asbestos, the characterization of worker exposures is highly important. Currently applied sampling techniques have been found to collect mostly agglomerated particles with individual fibers being rare (Dahm et al. 2015). However, it is suggested that this is because sampling was conducted on CNT release from a matrix (Dahm et al. 2015). Limited research of CNT release from a bulk powder has been conducted; data on results from this application of the sampling method are important because it cannot be determined if the method is selective to discriminate against individual fibers.

The currently proposed NIOSH 7402 method for CNT collection and characterization relies on a solvent based transfer process (Birch et al. 2016). It has been hypothesized that this transfer process may have an impact on the observed fiber morphology and size distribution.

The purpose of this project was to compare the morphology and size distribution of CNTs collected by two methods; the NIOSH 7402 method and using the Tsai Diffusion Sampler (TDS). The TDS collects particles onto a Transmission Electron Microscope (TEM) grid for direct analysis, in addition to a filter which can be observed using a Scanning Electron Microscope (SEM). This evaluation was based upon the number of fibers and fiber size distribution of samples collected on the filter and TEM grid for both samplers.

## CHAPTER 2: METHODOLOGY

### 2.1 Process

To determine the efficacy of each carbon nanotube sampling method, CNTs were generated through manual stirring inside of an enclosure placed inside of a glovebox equipped with ultra-filter. Experiments lasted forty minutes and stirring was conducted for fifteen minutes. The SMPS, OPS, TDS, and NIOSH 7402 sampler were placed on the wall of the enclosure and sampled directly adjacent to aerosol generation. The TDS (0.3 L/min) was placed the farthest away from the 7402 sampler (4 L/min) because of its significantly lower flow rate. The experimental setup is displayed in Fig. 1. Samples were only taken during the stirring period.

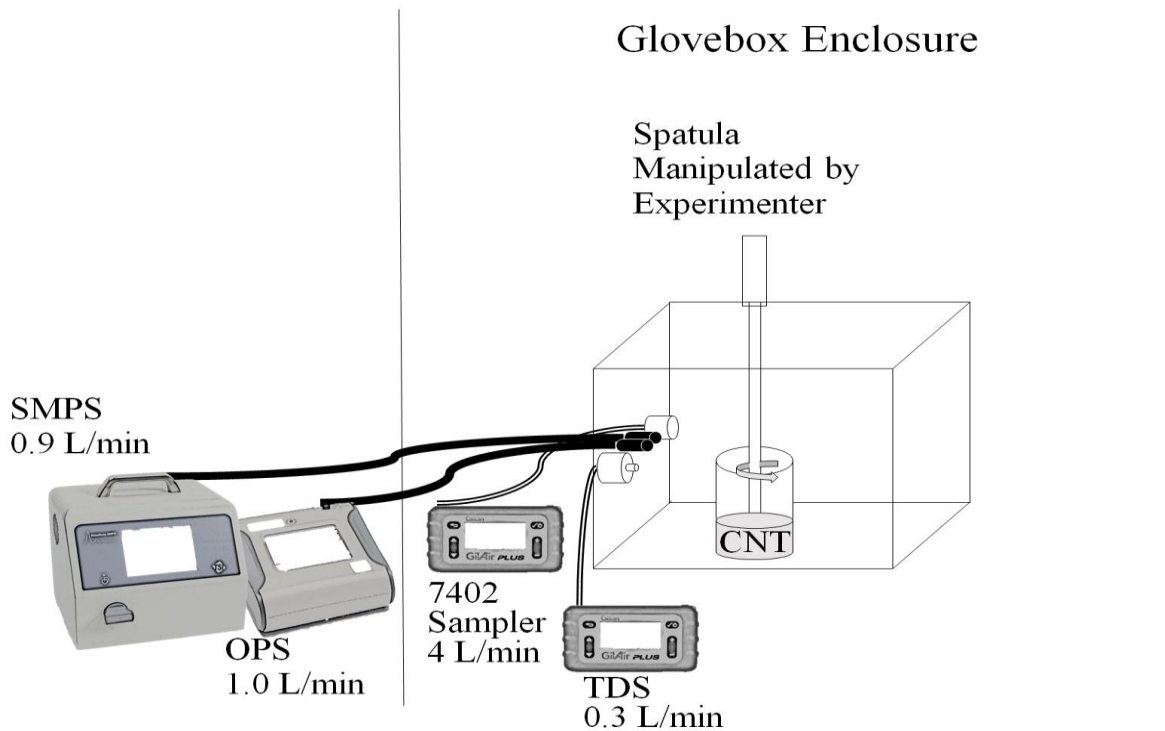


Figure 2-1: Experimental setup for CNT generation

## 2.2 Evaluation of Carbon Nanotube Collection

The efficacy of each sampler for collecting carbon nanotubes was evaluated using both TEM grids, and the filter used in sampling. The TDS collects CNTs directly onto a TEM grid which is attached to a polycarbonate filter with 0.2  $\mu\text{m}$  pores; this allows for nanoparticles and respirable particles to be collected simultaneously. Respirable particles are collected on the filter through impaction and nanoparticles are deposited on the grid using Brownian motion. The 7402 sampler uses a three piece, open-face cassette; it collects particles onto a mixed cellulose ester (MCE) filter with 0.45  $\mu\text{m}$  pores, and then requires particles to be transferred on to a TEM grid. In this study, both filters and grids from each sampler were analyzed.

TEM grids were imaged using a JEOL JEM2100F TEM at 200 kV. An image of each grid space was taken first, then images of every CNT in that grid space were taken. The microscope operator continued to take images of grid spaces until 100 structures were found. TDS samples were taken at a magnification of 5,000x to 15,000x, while 400x to 6,000x was used for samples prepared in accordance with NIOSH 7402. For both samples CNT structures were counted in accordance with the NIOSH 7402 method for CNT collection and analysis; all individual fibers with a  $>3:1$  aspect ratio were counted, and then clusters were characterized by their maximum crosswise dimension and then placed into size bins of  $< 1 \mu\text{m}$ ,  $1-2 \mu\text{m}$ ,  $2-5 \mu\text{m}$ ,  $5-10 \mu\text{m}$ , and  $> 10 \mu\text{m}$ . The crosswise dimension of each CNT cluster was measured using Gatan Digital Micrograph.

The collection filter from each sample was imaged using a JEOL JSM-6500F SEM at 15 kV. Images of each filter were taken at 1,500x, ten images were taken of each sample. Images were taken evenly from the edge to the center of the filter, to show the variation of particle collection.

### 2.3 Estimation of Airborne Fiber Concentration

The equation used to estimate airborne CNT concentrations from fiber counting on the TEM grids is presented in Fig. 2; this equation is typically used to calculate the estimated airborne concentrations for asbestos characterization. For the TDS an effective filter area of 415 mm<sup>2</sup> was used; a grid opening area of 1.37 x 10<sup>-3</sup> mm<sup>2</sup> was used, this number was obtained from the manufacturer. A grid area opening and effective filter area of 0.01 mm<sup>2</sup> and 385 mm<sup>2</sup> were used respectively. These values were obtained from the laboratory that prepared these samples.

$$\frac{CNT\ Structures}{cc} = \frac{\#CNT\ structures}{\# Grid\ Openings\ Counted} \times \frac{1}{Volume(L)} \times \frac{Effective\ Filter\ Area\ (mm^2)}{Average\ Grid\ Opening\ Area\ (mm^2)} \times \frac{1L}{1000cc}$$

Figure 2-2: Equation used for airborne concentration estimation

## CHAPTER 3: RESULTS AND DISCUSSION

### 3.1 Particle Counting and Concentration Extrapolation

Particle counting and concentration estimates were based on data collected from TEM images taken of each sample. Examples of images taken of TDS and NIOSH 7402 samples are shown in Fig. 3a and Fig. 3b respectively. CNT counting was conducted on one grid from each sample; in contrast to the numbers used for airborne concentration estimations, the total number of particles collected on each considered grid opening were used. The TDS collected 320 particles on four grid openings. Samples from experiment one and two only required one grid opening to attain 100 counted particles, while the sample from the third experiment required two grid openings to attain 100 counted particles. Of the fibers collected, 82 percent were individual fibers, 17 percent were clusters less than one micron in diameter, and one percent were clusters one to two microns in diameter. No fibers or clusters larger than two microns in diameter were observed on the TDS samples.

The NIOSH 7402 sampler collected 342 particles on twelve grid openings. The sample from the first, second, and third experiments required four, six, and two grid opening respectively to attain 100 counted particles. Of the fibers collected, one percent were individual fibers, 7 percent were clusters less than one micron in diameter, 19 percent were clusters one to two microns in diameter, 36 percent were clusters two to five microns in diameter, 24 percent were clusters five to ten microns in diameter, and 13 percent were clusters larger than ten microns in diameter. A comparison of the number and size of fibers collected by each sampler is presented in Fig. 2-4 and Table 2-1.

The significant discrepancy in the number of individual and submicron fibers collected by each sampler can likely be explained by the sampler design and flowrate used. The TDS has an

aerodynamic  $D_{50}$  of approximately  $4\mu\text{m}$ , this is determined by the inlet diameter and low flowrate designed for this use. The NIOSH 7402 sampler uses an open face cassette which allows it to collect fibers in the inhalable size range. Additionally, the TDS uses a polycarbonate filter with pores that are 200 nm in diameter compared to the NIOSH 7402 sampler which uses an MCE filter with pores that are 450 nm in diameter. Because of this, it is likely that particles smaller than the pore size are lost in the pores of the filter used by the 7402 sampler. The TDS also collects particles directly onto a TEM grid, while the 7402 method requires particles to be transferred onto a TEM grid using solvents. It is hypothesized that this process may have an effect on particle morphology.

Based upon the number of CNT structures collected in all size ranges, an airborne concentration estimate was calculated. This number is based upon the number of grid openings required to count 100 structures. The average estimated airborne concentrations calculated based upon the samples collected by the TDS and NIOSH 7402 sampler were  $5,200 (\pm 2,100)$  fibers/cm<sup>3</sup> and  $59 (\pm 9)$  fibers/cm<sup>3</sup> respectively. The large difference in estimated concentrations can be attributed to the additional number of grid openings required to count 100 CNT structures and the significantly larger volume of air sampled by the NIOSH 7402 sampler. As shown in Fig. 2-2, concentrations estimates are calculated by dividing by the volume of air sampled and the number of grid openings counted. As these variables increase, the estimated concentration decreases.

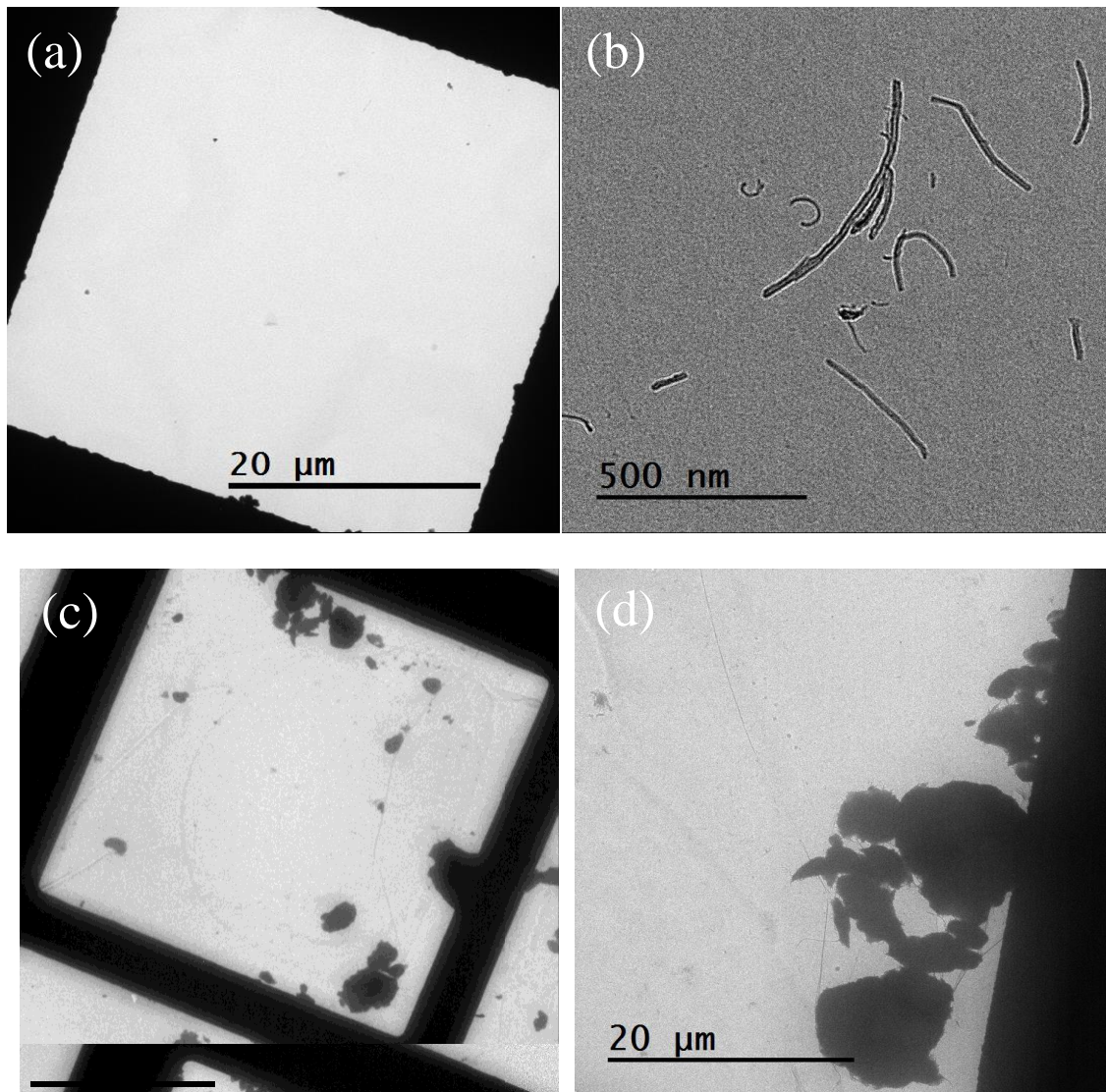


Figure 2-3: TEM images of sample grids. a) and b) TEM images of CNT samples collected by the TDS, c) and d) TEM images of CNT samples collected using the NIOSH 7402 sampler.

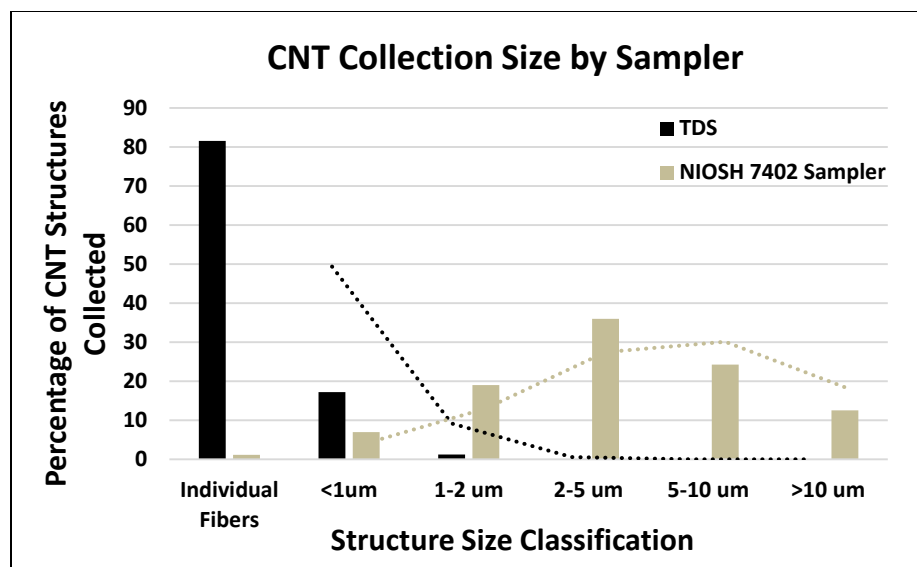


Figure 2-4: Histogram of percentage of fiber structures from TEM images collected by each sampler at each size category.

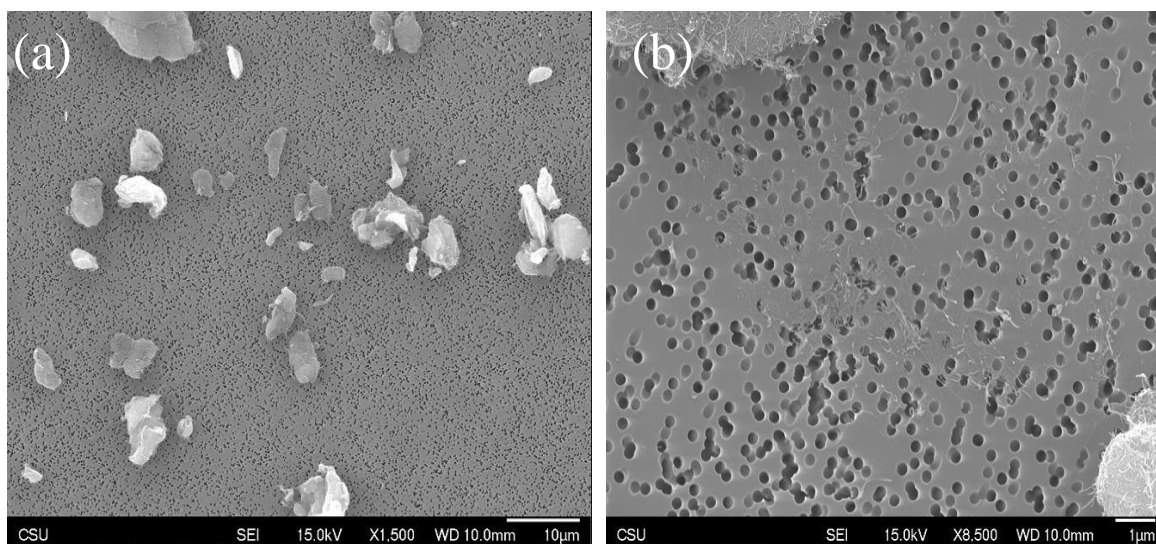
Table 2-1: Number of particles collected by each sampler in each size category

	Experimental Sample	Individual Fibers	<1um	1-2 um	2-5 um	5-10 um	>10 um
<b>TDS</b>	Sample 1	101	12	0	0	0	0
	Sample 2	79	26	0	0	0	0
	Sample 3	81	17	4	0	0	0
	Total Number of Structures	261	55	4	0	0	0
<b>NIOSH 7402 Sampler</b>	Sample 1	2	11	28	37	18	7
	Sample 2	0	6	17	41	29	16
	Sample 3	2	7	20	45	36	20
	Total Number of Structures	4	24	65	123	83	43

### 3.2 Qualitative Filter Analysis by SEM

The polycarbonate filter used by the TDS and MCE filter used by the NIOSH 7402 sampler were analyzed using SEM to examine the collected CNT fibers. Ten images were taken of each filter sample at 1,500x. A wedge shape filter was used, and images were taken at the edge, middle, and center. Examples of images taken by the SEM were presented in Fig. 5. It was observed that the filters collected by the NIOSH 7402 sampler had significantly more CNT structures than

samples collected by the other sampler. The majority of CNT structures found on this sampler exceeded 2 microns in diameter with many being in excess of 10 microns. This result was expected as this sampler uses a significantly higher flowrate than the other instruments present in the sampling enclosure, and thus collects more CNT structures on the filter. However, no individual fibers were identified on the MCE filters from this sampler. These results were somewhat consistent with the filter samples collected by the TDS. The majority of particles collected by the TDS also exceeded 2 microns in diameter; CNT clusters larger than 10 microns in diameter were common as well. In addition to larger CNT structures, individual fibers not found on the MCE filter were observed on the polycarbonate filter. They were observed on all three samples collected by the TDS. As discussed in the previous section, the lack of individual particles on the MCE filters collected by the NIOSH 7402 sampler is likely caused by the large pore size (450 nm in diameter) and higher flowrate. Because of this, there is a lower probability that individual nanofibers will be collected on the MCE filter. Additionally, CNT structures have a similar contrast to the MCE filter under the SEM. This makes visual identification of smaller structures on these filters difficult as shown in Fig. 2-5 c.



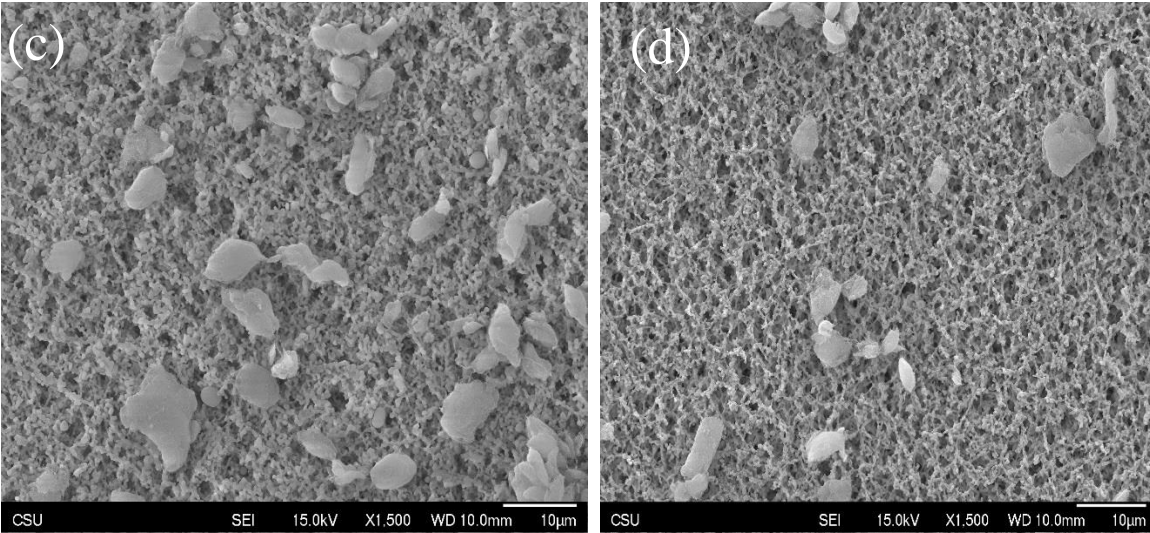


Figure 2-5: Examples of filter samples taken by SEM. a) and b) Images of the CNT structures collected on a polycarbonate filter by the TDS, c) and d) Images of CNT structures collected on a MCE filter by the NIOSH 7402 sampler.

### 3.3 Real-Time Instrument Measurements

Measurements were recorded by the SMPS and OPS throughout the entire experiment. It was found that concentrations were relatively consistent during all experiments. The average concentration measured by the SMPS during CNT generation was  $1,100 (\pm 25)$  particles/cm<sup>3</sup>. The average CNT structure concentration measured by the OPS during CNT generation was  $33 (\pm 4)$  particles/cm<sup>3</sup>. The relative D<sub>50</sub> measured by the SMPS and OPS were 116 nm and 522 nm respectively. Based upon the RTI data, it appears as though the majority of CNT structures generated were less than 200 nm in diameter. CNT structure concentration over time as measured by the SMPS and OPS are presented in Fig. 6.

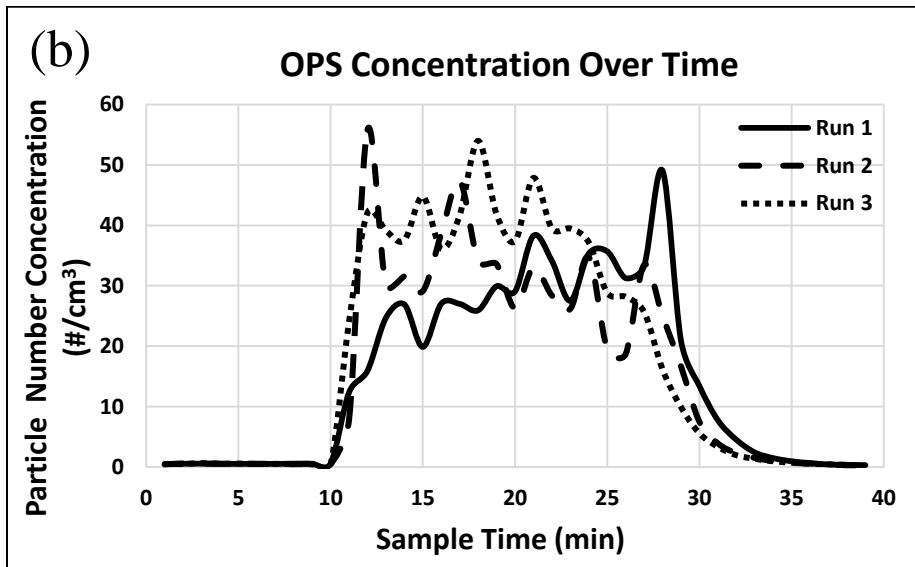
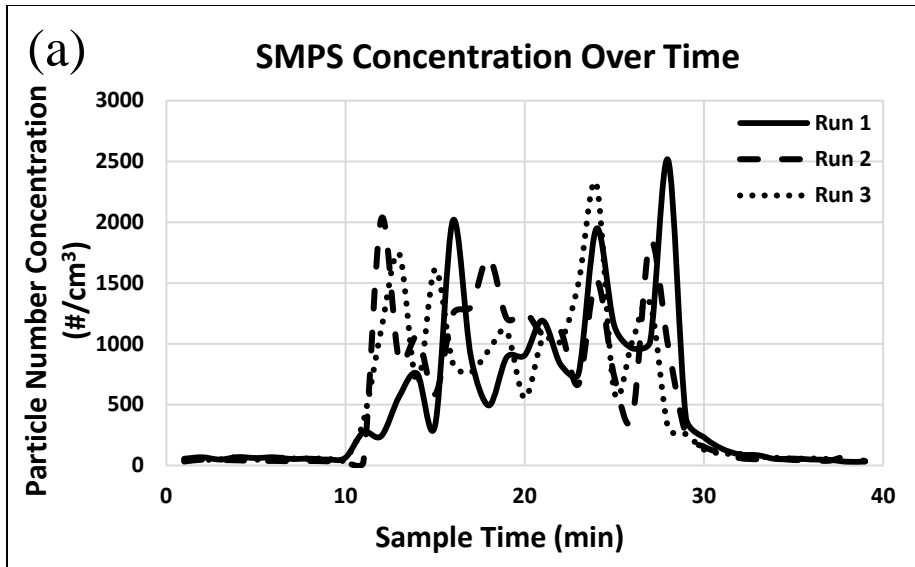


Figure 2-6: Particle concentration over time measured by the real-time instruments. a) Airborne particle concentration over time measured by the SMPS, b) Airborne particle concentration over time measured by the OPS.

## CHAPTER 4: CONCLUSION

In this study, two CNT sampling methods were compared to determine the particle morphology and size distribution collected by each. This evaluation was based upon the counting method used by the proposed NIOSH 7402 method for collecting CNTs, and calculations used to estimate the airborne concentrations from samples collected on TEM grids. Additionally samples collected onto filters were also compared. It was found that the TDS, which collects particles directly onto a TEM grid and polycarbonate filter, primarily collected individual fibers and CNT structures smaller than one micron in diameter. The average estimated airborne concentration based upon the samples collected by this sampler was 5,200 fibers/cm<sup>3</sup>. The NIOSH 7402 sampler, which collects particles onto a filter and then uses a solvent-based process to transfer particles onto a TEM grid, mostly collected particles larger than two microns in diameter. The average estimated airborne concentration based upon the samples collected by this sampler was 59 fibers/cm<sup>3</sup>. These findings were corroborated by the images of filters taken by the SEM. While the majority of all particles collected on the filters of both samplers were larger than two microns in diameter, small CNT structures and individual fibers were observed on the samples collected by the TDS. This was not seen on the samples collected by the NIOSH 7402 sampler. Additionally, the measurements collected by the real time instruments suggest that concentrations significantly exceeded those estimated by the NIOSH 7402 sampler. While these instruments are not completely accurate, they can reasonably assess airborne concentrations of contaminants.

The purpose of the fiber samplers compared in this study is to ultimately assess worker exposures to CNTs. This exposure assessment data is then used to make personal protective equipment and administrative decisions to ensure worker safety. Based upon the data, it was found that the sample collected by the TDS estimated a significantly larger airborne concentration than

the sample collected by the NIOSH 7402 sampler. Because of this, it is recommended that the TDS sampler be used as the information collected by it would warrant a more conservative approach to worker safety and health.

For the data collected by each sampler to be useful, a disease end point needs to be established based upon a specific exposure level. This would require comprehensive data on cell toxicity, animal exposure, and human exposure through epidemiological studies. From this information, an evidence based occupational exposure limit could be implemented based on the severity of the disease outcome and dose required to elicit this response. Future studies should also be aimed at further characterizing relationship between the data collected by each personal sampler and worker exposure.

## REFERENCES

- Bateson, T. F., Comba, P., Bugge, M. D., Debia, M. (2017). SOME NANOMATERIALS AND SOME FIBRES, IARC MONOGRAPHS ON THE EVALUATION OF CARCINOGENIC RISKS TO HUMANS, 35-214.
- Donaldson, K., Aitken, R., Tran, L., Stone, V., Duffin, R., Forrest, G., Alexander, A. (2006). Carbon Nanotubes: A Review of Their Properties in Relation to Pulmonary Toxicology and Workplace Safety, *Toxicological Sciences*, 5-22.
- Muller, J., Huaux, F., Moreau, N., Misson, P., Heilier, J.-F., Delos, M., Arras, M., Fonseca, A., Nagy, J. B., Lison, D. (2005). Respiratory toxicity of multi-wall carbon nanotubes, *Toxicology and Applied Pharmacology*, 221-231.
- Lam, C.-W., James, J. T., McCluskey, R., Hunter, R. L. (2004). Pulmonary Toxicity of Single-Wall Carbon Nanotubes in Mice 7 and 90 Days After Intratracheal Instillation 126-134.
- Poland, C. A., Duffin, R., Kinloch, I., Maynard, A., Wallace, W. A. H., Seaton, A., Stone, V., Brown, S., MacNee, W., Donaldson, K. (2008). Carbon nanotubes introduced into the abdominal cavity of mice show asbestoslike pathogenicity in a pilot study, *Nature nanotechnology*, 423-428.
- Iijima, S. (1991). Helical microtubules of graphitic carbon, *Nature*, 56-58.
- Wang, X., Jia, G., Wang, H., Nie, H., Yan, L., Deng, X. Y., Wang, S. (2009). Diameter Effects on Cytotoxicity of Multi-Walled Carbon Nanotubes, *Journal of Nanoscience and Nanotechnology*, 3025–3033.
- Yamashita, K., Yoshioka, Y., Higashisaka, K., Morishita, Y., Yoshida, T., Fujimura, M., Kayamuro, H., Nabeshi, H., Yamashita, T., Nagano, K., Abe, Y., Kamada, H., Kawai, Y., Mayumi, T., Yoshikawa, T., Itoh, N., Tsunoda, S.-i., Tsutsumi, Y. (2010). Carbon Nanotubes Elicit DNA Damage and Inflammatory Response Relative to Their Size and Shape, *Inflammation*, 276-280.
- Dahm, M. M., Schubauer-Berigan, M. K., Evans, D. E., Birch, M. E., Fernback, J. E. (2015). Carbon Nanotube and Nanofiber Exposure Assessments: An Analysis of 14 Site Visits, *Annals of Occupational Hygiene*, 705-723.
- Birch, M. E., Wang, C., Fernback, J. E., Feng, H. A., Birch, Q. T., Dozier, A. K. (2016). Analysis of Carbon Nanotubes and Nanofibers on Mixed Cellulose Ester Filters by Transmission Electron Microscopy, *NIOSH Manual of Analytical Methods*.

LIST OF ACRONYMS

CNT.....	Carbon Nanotube
MCE.....	Mixed Cellulose Ester
NIOSH.....	National Institute of Occupational Safety and Health
OPS.....	Optical Particle Sizer
RTL.....	Real Time Instrument
SEM.....	Scanning Electron Microscope
SMPS.....	Scanning Mobility Particle Sizer
TEM.....	Transmission Electron Microscope
TDS.....	Tsai Diffusion Sampler